Getting over continent ocean boundaries

Graeme Eagles, Lucía Pérez-Díaz, Nicola Scarselli

PII: S0012-8252(15)30055-6
DOI: doi: 10.1016/j.earscirev.2015.10.009
Reference: EARTH 2181

To appear in: *Earth Science Reviews*

Received date: 1 June 2015
Revised date: 7 September 2015
Accepted date: 26 October 2015

Please cite this article as: Eagles, Graeme, Pérez-Díaz, Lucía, Scarselli, Nicola, Getting over continent ocean boundaries, *Earth Science Reviews* (2015), doi: 10.1016/j.earscirev.2015.10.009

Getting Over Continent Ocean Boundaries

Graeme Eagles, Lucía Pérez-Díaz, and Nicola Scarselli

Graeme Eagles*
Alfred Wegener Institute, Helmholtz Centre for Polar und Marine Research,
Am Alten Hafen 26,
27568 Bremerhaven,
Germany.

COMPASS Research Group,
Department of Earth Sciences,
Royal Holloway University of London,
Egham, Surrey,
TW20 0EX,
UK.

geagles@awi.de

Lucía Pérez-Díaz
COMPASS Research Group,
Department of Earth Sciences,
Royal Holloway University of London,
Egham, Surrey,
TW20 0EX,
UK.

Nicola Scarselli
Fault Dynamics Research Group
Department of Earth Sciences,
Royal Holloway University of London,
Egham, Surrey,
TW20 0EX,
UK.

*Corresponding author

Abstract

The idea of a simple linear boundary between continental and oceanic crust at extended continental margins is widely recognised to be an oversimplification. Despite this, such boundaries continue to be mapped because of their perceived utility in palinspastic and plate kinematic reconstructions. To examine whether this perception is justified, we review the data and models on which basis continent ocean boundaries are interpreted, and map a set of such interpretations worldwide from more than 150 publications. The maps show that the location of the continent ocean boundary is rarely consistently estimated within the ~10—100 km observational uncertainty that might be expected of the geophysical data used for doing so, that this is the case regardless of whether the transition zone behind the boundary is classified as magma rich or magma poor, and that the geographical separation of estimates exceeds the width of single-study continent ocean transition zones. The average of global maximum separations across sets of three or more estimates is large (167 km) and mostly a consequence of interpretations published over the last decade. We interpret this to indicate an extra component of uncertainty that is related to authors' understanding of the range of features that are interpretable at extended continental margins. We go on to discuss the implications of this uncertainty for palinspastic and plate kinematic modelling using examples from the literature and from the South Atlantic ocean. We conclude that a precise continent ocean boundary concept with locational uncertainty defined from the ensembles is of limited value for palinspastic reconstructions because the reconstruction process tends to bunch the ensemble within a region that is (i) of similar width to the observational uncertainties associated with continent ocean boundary estimates, (ii) narrower than the regions of uncertainty about rotated features implied by the propagation of uncertainties from plate rotation parameters, and (iii) coincident, within all the above uncertainties, with the more-easily mapped continental shelf gravity anomaly. Secondly, we conclude that estimated continent ocean boundaries are of limited use in developing or testing plate kinematic reconstructions because (i) reconstructions built using them as markers do not, within uncertainty limits defined from the ensembles, differ greatly from those using more-easily determined bathymetric or gravity anomaly contours, and (ii) because it is impossible to segment and date them with useful precision to use as markers of the edges of rigid oceanic lithosphere outside of the constraints of a pre-existing plate kinematic model.

Keywords

continent ocean boundary; continent ocean transition; extended continental margin; marine geophysics; palinspastic reconstruction; plate motion

Introduction

The continent ocean boundary (here COB, but also widely abbreviated to OCB in the literature) is a well-known concept in global tectonics. It is recognised to distinguish distinctive continental and oceanic crustal types (e.g. Wegener, 1915; Holmes, 1931; 1944). Before plate tectonics, little detailed attention was paid to the processes that might have led to the formation of COBs (e.g. Drake and Kosminskaya, 1969). Later, it became evident that COBs might form as a result of processes associated with relative plate motions that are divergent, convergent or conservative. Particular attention has been devoted to the continental margins that are generated in plate divergence, because they contain a record of relative plate motions and because they are the sites of thick accumulations of sediments and hydrocarbon reserves. Margins of this kind are generated by extension and rupture of continental crust and the subsequent eruption of igneous rocks next to and/or over the extended region.

Despite the recognition of processes involved in extended margin formation, the COB concept remains a matter of observing the contrast in crustal type, from continental to oceanic, across such a margin. With this binary classification, the COB can be portrayed on maps as a line generated from observations in geophysical data. Its uncertainty might therefore conceivably be related to the resolution of geophysical data it is observed in. Those data, however, regularly reveal the presence of features that might plausibly be assigned to either continental or oceanic crustal type (e.g. Ball et al., 2013). Reflecting this, some maps portray a finite-width continent ocean transition zone (here COTZ, but in the literature alternatively abbreviated as COT or OCT), instead of a linear COB. The COTZ can thus be considered as a cartographic manifestation of another kind of uncertainty, that is, in crustal structure and composition. This uncertainty depends not on the resolution, but the interpretation, of geophysical data at extended continental margins. To illustrate the importance of this, Whitmarsh and Miles (1995) listed three possible interpretations of the COTZ. The first is as heavily intruded continental crust buried by extrusive material, implying a COB at its distal extreme (Boillot and Froitzheim, 2001; Blaich et al., 2011; Lundin and Doré, 2011). The second interpretation, of a mixture of exposed upper mantle and

volcanic products of ultraslow seafloor spreading, implies a COB at its proximal extreme (e.g. Roots et al., 1979; Mjelde et al., 1997; Scott, 2000). The third interpretation considers the COTZ to consist of continental crustal blocks surrounded by upper mantle material that has been exposed during mechanical removal of the crust by faulting. A unique linear COB is impossible to define in this context.

Here we review the observational basis for mapping COB and COTZ features in time and space, considering the related component of uncertainty in their dating and locations. We go on to present a compendium of COB and COTZ interpretations for various extended continental margins worldwide. We use the compendium to estimate the interpretational component in locational uncertainty for the COBs, and compare it to the extents of mapped COTZs. Finally, we briefly discuss the importance of these uncertainties in the context of tasks that COB estimates are commonly set to.

Definition and demarcation of the COTZ and COB

Demarcation of the COB is based on geophysical observation and interpretation. To focus this task, many authors make a first order classification of COTZs on the basis of melt supply. At some COTZs, seismic data can be interpreted as showing the upper mantle to be exposed at the seabed or directly overlain by sediments (Reston, 1996). Referring to the often absent or stunted igneous crust above the mantle, these transitions are often referred to as magma poor. Understanding of this margin type is based on geophysical and drill core data from the conjugate margins of Iberia and Newfoundland, and studies of presumed analogues in the Alps (e.g. Boillot et al., 1987; Whitmarsh et al., 1996; Manatschal and Nievergelt, 1997; Tucholke et al., 2004; Sutra et al., 2013). Based on this work, the basement at these margins is dominated by mantle lithologies, from whose geochemically determined continental or oceanic affinities the COB can be interpreted. The result is not unambiguous (e.g. Seifert et al., 1997). In contrast, at so-called magma rich transitions, a largely seismically isotropic crust of up to 20 km thickness can be present in the COTZ. This isotropy makes it possible to interpret the crust at such margins as igneous but, again, such interpretation cannot be considered unchallengeable.

Although the melt-supply classification scheme is widely used, its application too is a matter of interpretation, as conflicting studies illustrate for the southern Australian and South Atlantic Santos Basin margins (e.g. Ball et al., 2013; Blaich et al., 2011; Fromm et al., 2015; Klingelhöfer et al., 2014). Consequently, both magma rich and magma poor COTZs have been interpreted as the equivalents of oceanic crust generated under unusual melting conditions (Williams et al., 2011; Scott, 2000; Gillard et al., 2015) or as the products of extreme volcanic or mechanical alteration of continental crust and mantle occurring prior to the onset of seafloor spreading (Eldholm and Grue, 1994; Lundin & Doré, 2011; Nirrengarten et al., 2014). By different interpretation of the same observations, therefore, a COB at any extended margin could plausibly be mapped anywhere between the oceanic and continental extremes of its COTZ.

COB and COTZ in seismic reflection data

Depending on the experiment set up, goals, and acquisition conditions, reflection seismic data might image down as deep as the acoustic basement or through the whole crust. Based on seafloor mapping, drilling, and ophiolite studies, the oceanic crust is considered to consist of melt products intruded as massive bodies, dykes, and sills, and extruded as pillow lavas, hyaloclastites, and blocky flows from fissures and central volcanoes (Moores and Vine, 1971; Small, 1998). As this arrangement is strongly three-dimensional and the melt products are largely of invariable composition, one way of interpreting the presence or absence of oceanic crust is thus to map reflections from the top surface of acoustically-transparent basement. The surface should be uneven and a source of numerous diffractions, consistent with a covering of basalt lava flows. In locations near continental margins, such a reflector is likely to be overlain by nearly flat parallel reflections from deep ocean sediment layers. This kind of seismic stratigraphy is consistent with the presence of oceanic crust but may not be diagnostic of it; mature volcanic rift zones may also host large lakes or ocean bights where similar relationships can develop on continental crust. An alternative or complementary interpretation in the acoustic basement is of normal faults, which are taken to indicate the extension of pre-existing, and therefore continental, crust as a mechanism to compensate for plate divergence. However, it is understood that normal faulting is a prominent process in the formation or alteration of oceanic crust too (e.g. White et al., 1990).

In surveys where greater depth has been imaged, prominent flat or gently dipping surfaces several kilometres beneath basement are widely interpreted to indicate the base of oceanic crust. This kind of interpretation is also made with reference to ophiolite analogues in which strong acoustic contrasts are attributable to the cumulate textures formed near the bases of massive gabbroic bodies, which in turn are interpreted to represent the floors of magma chambers from which the oceanic crust forms. The COB has been placed at the landward limits of these reflectors or at vertical steps in them (e.g. Stagg et al., 2004; Leitchenkov et al., 2014). Without high-resolution velocity models these interpretations are not unique because the crust or the upper mantle may also display reflections. Based on such observations, Rosendahl et al. (1992) suggest alternative interpretations in terms of the brittle-ductile transition and/or presence of melt products at various depths and distances within a complex COTZ. Similarly, studies targeting magmatic processes at active mid-ocean ridges have shown that the distribution of lower- and base-crustal reflectivity within the oceanic crust is patchy and, where present, its topography can be complex (Muller et al., 1999; Singh et al., 2006a,b; Canales et al., 2009). The latter is a foreseeable consequence of the observed 0-8 km global variability in the thickness of unequivocal oceanic crust and of the interpreted 0-30 km variability in the crustal thicknesses of what may also be igneous crust in COTZs and oceanic large igneous provinces (Laske et al., 2013; Mjelde et al., 1997; White et al., 2001; Dick et al., 2003).

Assuming despite this that the observational criteria of faulted acoustic basement, rough unfaulted acoustic basement and bright deep reflectors do reliably indicate the presence of continental and oceanic crust, it is useful to notice that the distances along profile over which they each appear do not usually coincide. This can be taken advantage of to suggest an observational uncertainty for COBs determined from seismic reflection data. In Figure 1, a basement reflector that is offset by normal faults, suggesting it may be interpreted as continental crust, is separated by around 70 km from a deep reflector interpreted as the base of the oceanic crust. The COB could lie somewhere along this distance. In the same survey data set, Stagg et al. (2004) showed offsets of ~40 km (their figure 5) and ~100 km (their figure 9) for COBs defined with interpretations of normal faulting and base-of-crust, and one of 20 km based on rough basement and base-of-crust interpretations (their figure

10). With these examples, a mean picking uncertainty of around 50 km within a range of 10-100 km seems appropriate for COBs determined from seismic reflection data alone.

Seismic reflection data in magma rich COTZs exhibit prominent packages of seaward dipping reflectors (SDRs; e.g. Figure 2). Most authors relate SDRs to the presence of thick sequences of basalt that effused subaerially and subsequently weathered to generate strong acoustic impedance contrasts with the bases of their overlying flows. The eponymous dip is attributed to basalt effusion over extended continental margins and/or the neighbouring ocean whilst the young oceanic crust is undergoing rapid subsidence (Gladczenko et al., 1997; Planke and Eldholm, 1994). With this interpretation it might be thought suitable to use SDRs for temporal definition of the presence of oceanic crust between a diverging plate pair, although the presence of multiple SDR wedges at some margins (e.g. Planke et al., 2000) challenges the intuitive attraction of doing so. With the same caveat, the interpretation also implies that SDR sequences can be used to demark the COB. The mapped widths of SDR packages vary in the range 50-150 km, which can be taken as a maximum value for the observational error in COB estimates made with specific reference to them.

COB and COTZ in seismic refraction data

Seismic refraction data can be obtained from individual sonobuoys as point estimates for columns sampling layers of variable thicknesses and velocities, or with greater accuracy from lines or arrays of ocean bottom seismometers (Figure 3). These data can be used to constrain the COB on the basis of an expectation that the seismic velocity of the igneous oceanic crust below its pillow lava layer is relatively constant at >5.8—6.0 kms^{-1}, and that its usual thickness does not vary greatly beyond 7-8 km (e.g. Christensen and Mooney, 1995). The horizontal resolution of refraction data made with closely spaced ocean bottom equipment is sufficient to show that these velocity conditions might come to be met over a zone of ~40-100 km width (e.g. Voss et al., 2007). The uncertainty of sonobuoy based COBs, however, more strongly depends on the geographical spacing of sonobuoys, which is irregular but usually large (>50 km).

Landwards of the relatively simple oceanic crust, magma rich COTZs exhibit more variability in their seismic velocities. Overall, their seismic velocity profile is intermediate between those for unequivocally continental and oceanic crust (e.g. Altenbernd et al. 2014). Often, seismically very fast bodies are imaged at the base of the crust. The fast velocities are attributed either to the presence of ultramafic cumulate rocks formed by excess melt production during breakup, or of eclogite formed by reburial of previously exhumed and hydrated upper mantle (Lundin and Doré, 2011). These contrasting interpretations can be taken to imply different COB locations at the inner or outer edge of the COTZ. In contrast, magma poor COTZs may show areas of fast upper mantle velocities interspersed among islands of somewhat slower velocity. This is usually interpreted with reference to obducted field analogues in terms of the detachment and separation of blocks of hyperextended lower continental crust along nearly horizontal shear zones (e.g. Manatschal, 2004).

COB and COTZ in magnetic data

Hemant and Maus (2005) showed that the vertically integrated susceptibilities of oceanic and continental crust are in most places quite similar, such that COBs should not be expected to raise diagnostic magnetic anomalies at long wavelengths. This is not the case for the upper crust, however, so that at shorter wavelengths magnetic data might be expected to show a magnetic anomaly related to the transition from continental to oceanic crust. Such anomalies indeed appear at some sheared continental margins. Before drilling led to a better appreciation of the reasons for the acoustic impedance contrasts that give rise to SDRs at extended margins, some of the magnetic anomalies associated with SDRs were also attributed to a crustal susceptibility contrast edge effect at extended continental margins (Rabinowitz and LaBrecque, 1979). Since then, it has become clear that edge effect anomalies are not ubiquitous features of extended continental margin segments. This can be understood as a consequence of the presence of intrusive rocks in the upper continental crust of COTZs, which makes it difficult to distinguish magnetically from the igneous oceanic crust (e.g. Gernigon et al., 2015).

Magnetic polarity reversal isochrons can be used to map areas of unequivocal oceanic crust reliably because there are no continental processes that consistently lead to close mimicry of the distinctive great circle-shaped polarity edge effect anomalies that form over oceanic

crust during stable seafloor spreading. Where reversal intervals are wide, for example if they formed during long periods of stable geomagnetic polarity like the Cretaceous Normal Polarity Superchron, then the lack of edge effects makes the magnetic anomaly signature of the oceanic crust less distinctive. In other circumstances, for example in oceanic crust formed at sediment-covered spreading centres (Levi and Riddihough, 1986) or at ultra slow spreading rates (Jokat and Schmidt-Aursch, 2006), or at short lengths of mid-ocean ridge crest, these anomalies may be less reliable diagnostically.

Into COTZs, the magnetic anomaly field over SDR bodies can show similarities to those raised by the basalt layer in oceanic crust. This permits interpretation of the anomalies as signals of entirely igneous crust in magma rich COTZs, albeit not unequivocally. The linear magnetic anomalies related to SDR sequences such as those in the South Atlantic may approach or exceed 100 km in width. If they exhibit polarity reversals, then the reversals have low-angle limbs, because of the tapering source geometry. Figure 4 compares a set of such records to oceanic magnetic reversal anomalies. The absolute picking error in the magnetic anomaly related to a SDR wedge will be greater than that associated with picking a reversal anomaly isochron whose source is a magnetization vector contrast that is closer to vertical. From forward consideration of source body geometry, navigational error, and misfits in plate kinematic models, typical uncertainties assumed or calculated for oceanic reversal isochron anomalies are in the region of 3-10 km (Kirkwood et al., 1999; Eagles, 2004). Picking the equivalent part of a SDR-related anomaly, on the other hand, may be prone to an error of 20-50 km.

COB and COTZ in gravity data

Tectonic extension and processes related to it give rise to broad gravity anomaly patterns at continental margins (Watts and Fairhead, 1999). These patterns are dominated by the effect of the strong and shallow density contrast between rocks and sea water at the continental shelf edge, but also respond to density contrasts related to the three dimensional distributions of sediments, of oceanic and continental crust, of the shallow mantle beneath thinned continental crust, of underplated gabbro, and of exposed or shallow subcropping mantle rocks at magma poor margins. Watts and Fairhead (1999) showed that either the free air gravity high (e.g. at the Baltimore Canyon margin) or its

seaward low (e.g. at the Congo margin) can be related to the COB, as the anomaly varies in relation to the margin's strength and flexural response to the sedimentary and underplating loads (Figure 5). Continental edge gravity anomalies are therefore unlikely to consistently show the precise location of the COB, but can be used to interpret the locations of a variety of features that have been related to it in various ways.

Despite this, some studies apply specific interpretations of gravity anomalies at continental extended margins regionally or globally. Rabinowitz and LaBrecque (1977) interpreted isostatic residual gravity anomaly highs in terms of scarps of oldest oceanic crust that are supported out of isostatic equilibrium by neighbouring more buoyant continental crust. The features they observed have since been noted to coincide with SDR sequences, which as we have seen are taken by some authors as COB indicators (e.g. Franke et al., 2006; Pawlowski, 2008). Lawver et al. (1998) and Macdonald et al. (2003), on the other hand, took the inner high of the continental margin-related free air gravity anomaly as a global proxy for the outermost limit of unequivocally continental crust. Acknowledging this is unlikely to be accurate at prograded margins, they maintained that it is admissible elsewhere in instances where the COB undergoes rotation as part of a plate reconstruction, because the uncertainty in the interpretation is usually smaller than the statistical uncertainty in the locations of features rotated in plate kinematic model rotations.

The products of transform faulting are readily interpretable from gravity data over the oceans (e.g. Sandwell and Smith, 2009; Sandwell et al., 2014). This process produces distinctive strike-slip fault zones that are active for a finite period whose duration depends on the plate divergence rate and length of the transform fault. This process leaves linear trough- and step-like traces in oceanic plate interiors called fracture zones that align in parallel sets along co-polar small circle trends. Transfer faults are tectonically similar features that may appear in continental extensional zones and have been suggested, locally, to continue as active offsets on divergent oceanic plate boundaries (Lister et al., 1986). The great majority of oceanic fracture zones, however, appear not to offset COTZs or to continue into them. In continental interiors, pre-existing rheological contrasts complicate the development of transform plate boundaries so that their traces anastamose via multiple strike-slip, reverse and normal fault segments to generate complex landforms. Fracture

zones reliably define regions of oceanic crustal development, and can be used to generate a conservative estimate of the landward edge of oceanic crust. Parts of Torsvik et al.'s (2009) COB estimates, from isostatic residual gravity anomaly textures in the South Atlantic, appear to make use of this observation. Fracture zones, however, as linear features with finite spacing, can only provide only a punctuated minimum estimate of the extent of oceanic crust.

The picking error of gravity based COB estimates is illustrated in Figure 5. In total, continental margin gravity anomalies may exceed 150 km in length and have multiple components. The most conservative value for the possible uncertainty in COBs picked from gravity anomalies might therefore be taken as 150 km, but this does not allow for the fact that the anomaly's individual components can be interpreted in terms of COBs. The picking error in any of these components (e.g. the seaward trough) is probably closer to 50 km. In comparison, the picking error for a fracture zone, such as commonly used in quantitative plate kinematic reconstructions, is around 5-10 km in the trough of a total anomaly that is typically 25-40 km wide (Müller et al., 1991).

COB as a plate kinematic prediction

Blaich et al. (2010) presented a COB location for part of the Atlantic margin of South America on the basis of rotating the geophysically-defined COB from its African conjugate. Making this kind of determination requires the choice of a set of Euler rotation parameters for the instant of continental breakup, an assumption that the geophysically-defined COB is an isochron, and an assumption that it is the conjugate of the feature being predicted. These assumptions contribute to the interpretational component of COB location uncertainty. The observational component of this uncertainty is a product of the propagation of the observational error or uncertainty in the location of the conjugate feature through the error in the Euler rotation, if it has been possible to calculate one. Experience suggests that the increase in uncertainty like this is unlikely to be less than around 20 km and, depending on the plate kinematic model geometry, may be several times that figure.

Why no process-based interpretation of the COB and COTZ?

In the above review, we have given no process-related definition of the COB. Such a definition does not exist, to our knowledge, in the literature. Similarly, we have given no unique process-related definition of the COTZ. The descriptions of the observations used to determine these features show that this is because the processes by which the oceanic crust forms and is altered in order to accommodate plate divergence (volcanism and normal faulting) also come to affect and eventually dominate the evolution and construction of the upper crust in continental extensional zones.

The Afar depression at the northernmost end of the East African rift zone and southernmost end of the Red Sea illustrates this. East of the footwalls of the main bounding rift faults, the depression is broad, low lying, and flat. The crustal thickness change across these faults implies a minimum stretching factor of about two (Tiberi et al., 2005), whereas plate kinematic modelling of the depression's formation suggests a factor of more than three (Eagles et al., 2002). These values straddle the range over which crustal extension is thought to give way to the generation of oceanic crust. The hanging walls of the faults are themselves strongly faulted by a dense network of normal faults that give rise to topography reminiscent of the abyssal hills of the deep oceans. A thick carpet of basalts and volcaniclastic rocks erupted at fissures and central volcanoes dominates the hanging wall stratigraphy. Wolfenden et al. (2005) suggested that these basalts are analogous to those that give rise to SDR sequences in mature COTZs. At deeper levels underlying the Afar depression, sills and dykes are generated in pulses known from periodic seismic crises (Rowland et al., 2007). In the upper mantle, tomographic studies reveal an area of partial melting (Bastow et al., 2005) that has delivered melt to significantly augment the crustal thickness (Hammond et al., 2011). Magnetic transects across the depression reveal paired magnetic anomalies that resemble the Brunhes-Matuyama transition flanking active mid-ocean ridges (Bridges et al., 2012).

Despite these similarities in process and product between its central region and a typical area of oceanic crust, it is not routinely concluded that oceanic crust underlies the Afar depression. Instead, studies point to the outcrop of extended lower continental crustal rocks around its margins, for example at the Ali Sabieh high, and note that the thickness and velocity profile of the crust do not resemble those of standard oceanic crust (e.g.

Hammond et al., 2011). Consequently, the crust in the depression is usually interpreted in terms of an actively forming COTZ, with multiple sites of volcanic addition to the margins of thinned and intruded continental crustal blocks lying beneath the depression's volcanic carpet. The crustal affinity of the Afar Depression is, put differently, unknown over a scale longer than the width of a typical oceanic divergent plate boundary. The same can be concluded of COTZs at extended continental margins. Defining COTZ extents, therefore, is a task that is likely to be affected by similar observational and interpretational challenges as defining the COB.

Age of the COB

COBs and COTZs cannot be dated directly without samples of volcanic rocks from them. This cannot be routinely achieved because of the deep-water setting and thick sedimentary cover of most extended continental margins. Because of this, COBs or lengths of them are only assumed to be isochrons to which proxy ages are attributed. As with the task of mapping the COB, the choice of proxy requires adherence to a model of continental breakup during plate divergence. In some studies, the development of the COTZ is related to excess volcanism that is promoted by the presence of warm or fertile mantle rocks beneath the divergent plate boundary. This excess volcanism may also affect the continental interior neighbouring the COTZ where it leaves large igneous provinces as accessible and dateable products. With this relationship in mind, the COB in such locations can be assigned the same age as its supposed equivalents on land (e.g. Torsvik et al., 2009). This kind of relationship has been proposed to date COBs in margins of the South, Central and North Atlantic, the NW Indian Ocean, west of Australia and southeast of Africa. Judging from dating of their products on land, the duration of the most voluminous periods of excess volcanism events rarely exceeds 5 Myr (e.g. Peate, 1997). This duration might serve as an estimate of the uncertainty of ages assigned to COTZs or COBs under the assumption that they are products of excess volcanism.

The timing of divergence of plates of oceanic lithosphere is recorded by linear magnetic anomalies. These anomalies are raised by contrasting remanent magnetization polarities in isochronous strips of basaltic crust formed by the action of mid-ocean ridges in a periodically reversing geomagnetic field. The anomalies are assigned ages by interpolation

between radiometric control points in magnetostratigraphic sequences. Uncertainties in these ages range between a few tens of thousands of years in Neogene rocks and <5 Myr in Mesozoic rocks (Gradstein et al., 2012). An age can be assigned to the COB by extrapolating from the age of the nearest of these isochrons, taking into account the distance between the two and the known rate of seafloor spreading after formation of the isochron. The distance for this extrapolation can be measured along a line drawn perpendicular to the oldest spreading anomaly or to the COB. Alternatively, it can be calculated using the plate divergence vector determined from a plate kinematic model. The calculation error associated with this process is proportional to the distance between the isochron and the COB estimate, and the confidence in any age estimate derived from it might be related to the variability in seafloor spreading rates in the earliest stages of ocean development. There is little reason to assume that the earliest rates were fixed or equal to later spreading rates, so it is not surprising that age estimates based on this technique do not always agree with ages determined from large igneous provinces. At the conjugate margins of southern Africa and Antarctica, COB ages estimated in these two ways differ by 16 Myr (Eagles and König, 2008). In many locations, including some bordered by large igneous provinces such as the Weddell Sea or South Atlantic ocean, multiple anomalies interpreted as magnetic reversal isochron sequences terminate obliquely at COB estimates such that the COB must be interpreted as a diachronous boundary (e.g. Rabinowitz and LaBrecque, 1979; Jokat et al., 2003). In such instances, any age applied to a COB estimate will be accurate at a single point only. In summary, in nearly all cases, sub-Myr precision in COB age assignment by consideration of magnetic isochrons cannot be justified.

In much tectonostratigraphic literature, the development of COBs is related to the development of regional stratigraphic discontinuities, often referred to as breakup unconformities (Falvey, 1974). As originally conceived, the breakup unconformity was thought to form at, and so pinpoint, a geological instant of strain localisation, continental rupture, failure, and wholesale subsidence of the continental margin coinciding with first emplacement of igneous crust between the diverging plates. In this view, rapid subsidence and the cessation of fault block rotations in the accommodation of plate divergence lead to the production of a prominent unconformity separating discontinuous fault-bounded strata below from continuous strata above. Dating of the breakup unconformity with these

assumptions thus implies dating of the COB, as both are products of the same process-event. By definition, unconformities are not directly dateable, but the sediments abutting them, where drilled, can be dated with the accuracies similar to those for chronostratigraphic timescales. This accuracy varies greatly depending on the accessibility of sections with good biostratigraphic frameworks and independently dateable strata to calibrate and interpolate them. Just 50% of Mesozoic stage boundaries are currently dated with a numerical estimate of precision, and these currently lie in the range 0.06—1.4 Myr (Gradstein et al., 2012). As breakup unconformities should not be expected to coincide with stage boundaries, however, the durations of Mesozoic stages (in the range 0.89—18.5 Myr) may serve as a more conservative estimate. Beyond this, regional unconformities are demonstrably not isochronous. On a regional scale, the underlying or overlying strata can be expected to have been deposited diachronously during margin progradation on timescales of the order of 10^5 years (Burgess and Hovius, 1997) or to be omitted in hiatuses of multi-million year duration (Kyrkjebø et al., 2004). What is more, at some margins the stratigraphic distribution of normal faulting or other indicators of crustal extension may leave it unclear which of a number of surfaces should be regarded as a margin's breakup unconformity (e.g. Del Ben and Mallardi, 2004; Ball et al., 2013), or indeed whether any such unconformity exists (Bosworth and Burke, 2005). Taking all this into consideration, although the uncertainty in unconformity-based COB dating may be as small as a hundred thousand years in exceptional cases, in most others it is likely to approach or exceed 5 Myr.

Locational uncertainties of COBs from interpretation ensembles

Above, we showed that demarcation of the COB is a task of observation and interpretation that is undertaken in and across various data sets. For the kinds of data sets reviewed here, the observable-related errors and uncertainties are mostly in the range 10-100 km, averaging around 50 km. If these factors dominate the uncertainty in mapping COBs, then we would expect any set of independent determinations of COB locations to cluster into a ~50 km wide group at any given margin. If however the uncertainty related to interpreting the COB within those data sets dominates, then we would expect groups of COB locations to distribute more loosely about a greater mean value. The larger this value comes to be, the less meaning we can expect to attach to the COB concept and its testimony. We describe these issues in the following, by mapping sets of features that have been labelled

as COBs, or whose definition is similar to that of COBs (e.g. Heine et al's (2013) 'Landward Limit of Oceanic Crust' or the seaward limits of published COTZs) for various extended margins globally. In some of the maps, we also compare the range of COB estimates to interpreted COTZ extents from the literature. We expect that if COTZs are conservatively estimated using the various data types reviewed above, then their widths might reasonably be expected to resemble or exceed the widths of the corresponding ensembles of COBs. If, on the other hand, COTZs are also subject to large interpretation bias, then we might expect published COTZs to be narrower than the COB ensembles.

Gulf of Mexico

The long time series (30 years) of COB estimates in the Gulf of Mexico, made using numerous independent data sets, is a consequence of political and economic stability and the region's status as a focus of hydrocarbon exploration and production. COB estimates have been made on the basis of all the main data sources described above, by numerous researchers and groups. Bird et al. (2005) presented eight COB interpretations alongside their own estimate. The ensemble we present in Figure 6 consists of all of those interpretations along with a number of others (Buffler and Sawyer, 1985; Ross and Scotese, 1988; Winker and Buffler, 1988; Sawyer et al., 1991; Salvador, 1991; Buffler and Thomas, 1994; Hall and Najmuddin, 1994; Marton and Buffler, 1994; Pindell, 1994; Schouten and Klitgord, 1994; Bird et al., 2005; Bouysse et al., 2009; Seton et al., 2012; Hudec et al., 2013; Christeson et al., 2014; Sandwell et al., 2014). In the areas of closest agreement, the COBs cluster over a distance of 70 km. The extreme interpretations of COB location are separated from one another by nearly 400 km. From 33 equally-spaced measurements along lines drawn for the shortest distance across those parts of the ensemble with more than three members, the mean of the maximum separations of COB estimates is 153 km and their standard deviation is 86 km (Table 1). Offsets between pairs of estimates are not constant, suggesting there is no overwhelming tendency for differing data sets to highlight different features within the COTZ for interpretation as the COB. For example, Bird et al.'s (2005) COB is located most proximally in the western part of the gulf, but it transects the ensemble to become the second-most distal estimate in the east.

Indian Ocean margins of Antarctica

The history of plate boundary development in the Indian Ocean is complex and has left much of its abyssal plain unsuitable for the direct plate reconstruction techniques that unite conjugate magnetic anomaly pairs (e.g. Hellinger, 1981). In addition, the availability and quality of magnetic isochron data are in many parts poor, and great lengths of the extended continental margins parted during the Cretaceous Normal Superchron to leave no linear magnetic reversal isochrons near them to unite. Consequently, interpretations and treatments of the ocean's COBs as conjugate isochrons have played a particularly important role in paleogeographic and plate kinematic reconstructions of the Indian Ocean in general, and the divergence of Antarctica from India and Australia in particular (e.g. Veevers, 2009; Williams et al., 2011; Gibbons et al., 2013).

Figure 7 shows a set of seventeen COB interpretations and one COTZ interpretation for the Indian Ocean margins of Antarctica made by interpreting magnetic, gravity, seismic reflection and refraction data (Powell et al., 1988; Royer and Sandwell, 1989; Eittreim, 1994; Ishihara et al., 1999; Gaina et al 2003; 2007; Stagg et al 2004; Leitchenkov et al 2009; 2014; Close et al., 2009; Direen et al., 2011; Seton et al., 2012; Ball et al 2013; Nogi et al 2013; Bouysse et al., 2009; Gohl, 2008; Gillard et al., 2015). Gillard et al. (2015) interpreted linear features they titled 'continental crust termination' and 'first steady state magmatic oceanic crust' that, in spite of their consideration of the intervening region as area created (not altered) during plate divergence, we would expect other interpreters to treat as proximal and distal COB estimates. In places where three or more estimates are mapped, the closest agreement between them is ~50 km for a short length of the continental margin off Terre Adélie. This segment is widely portrayed in plate kinematic studies as a sheared margin. Away from this segment, the largest separations are in the range 400-500 km, off Lützow-Holm and Prydz bays. Overall, the mean interpretational uncertainty defined by the maximum spacing in parts of the ensemble with three or more members, measured on 14 separate lines, is 206 km and the standard deviation is 93 km (Table 1). Similar to this, Ball et al. (2013) estimated COTZ widths in the range 110-310 km using profiles over five segments of the conjugate margins of Antarctica and southern Australia. They suggested that the COTZ formed diachronously over a period of 66 Myr. Direen et al. (2011), on the other hand, mapped a COTZ that is consistently narrower than the COB ensemble (Figure 7).

Leitchenkov et al's (2014) COB, interpreted from multiple data sets, and Seton et al's (2012) COB, whose data basis is not stated, are notable in this ensemble because they each represent the most distal COB estimate in some locations and the most proximal in others. As in the Gulf of Mexico, this transection suggests that the various techniques and data sets being used to generate COB estimates do not systematically sample different process-related features that form at different times or distances from the continental interior during the development of an extended continental margin.

Australia

Figure 8 shows an ensemble of more than twenty COB estimates for the extended continental margins of Australia (Veevers et al. 1985; Veevers, 1987; Powell, 1988; Stagg and Willcox, 1992; Exon et al., 1996; Fullerton et al., 1989; Royer and Sandwell, 1989; Royer and Rollet, 1997; Gaina et al., 1998; Brown e al., 2003; Norvick, 2004; Heine and Müller, 2005; Müller et al., 2005; Norvick et al., 2008; Bouysse et al., 2009; Direen et al., 2011; Williams et al., 2011; Seton et al., 2012; Ball et al., 2013, Hall et al., 2013; Gillard et al., 2015). Gravity-based interpretations are all made on satellite-derived data of the kind presented by Sandwell and Smith (2009) or Sandwell et al. (2014). Interpretations of these data dominate for the NW shelf, and as might be expected they agree well with one another. On the NW shelf, the ensemble's mean width on 16 profiles is 86 km, and its standard deviation is 110 km (Table 1), largely owing to differing interpretations of the crustal type at the Wallaby plateau.

There are larger disagreements between interpretations based on gravity data and other data sets, of which there is a greater variety on the south Australian margin. Notably, here, there is no significant seismic refraction data set. The largest uncertainty based on this part of the ensemble is in the region of 250 km, south of the Naturaliste Plateau. The mean of estimate separations in parts of the ensemble with more than three members on the southern margin, from 18 profiles, is 187 km, and the standard deviation is 80 km (Table 1). In addition, on this margin there is one mapped COTZ interpretation, from Direen et al. (2011). Like its Antarctic conjugate, this interpretation is of a COTZ that is narrower (range 15—120 km) than the COB ensemble (range 30—300 km). Ball et al.'s (2013) alternative

interpretation, although not presented in map form, suggested a slightly wider range of COTZ width, which is nevertheless still considerably narrower than the ensemble.

South China Sea

Like the Gulf of Mexico, the South China Sea is a small ocean whose margins have been extensively explored by the hydrocarbon industry. In contrast, much of the exploration in the South China Sea has been completed over the last decade. Because of this vintage, the data quality might be expected to be high and the COB locations consequently in closer agreement with one another. Figure 9 shows this region's ensemble of fifteen COB locations and two COTZs (Briais et al., 1993; Nissen et al 1995; Hsu et al., 2004; Wang et al., 2006; Hu et al., 2009; Bouysse et al., 2009; Deng et al., 2012; Li et al., 2012; Seton et al., 2012; Zhu et al., 2012; Barckhausen et al., 2014; Chen et al., 2014; Hwang and Chang, 2014; Pichot et al., 2014; Bai et al., 2015; Cameselle et al., 2015; Li et al., 2015). The mean ensemble width, measured on thirty profiles, is 118 km and their standard deviation is 92 km (Table 1). These statistics might be interpreted, as suggested above, in terms of recent high-quality data that promote a self-consistent set of COB interpretations. However, it is perhaps more revealing that most of the margin is delineated by just three or four COB estimates, and that the maximum separation of estimates (317 km) is located where all fourteen estimates coincide in the area SW of Taiwan. The widths of the published COTZs and the ensemble in this part of the margin significantly exceed the width of the COB ensemble elsewhere, suggesting much of the ensemble may not be a conservative representation of COB uncertainty. Overall, therefore, these observations support the idea that COB uncertainty is dominated by interpreter choices, rather than navigation or data resolution.

Northern Indian Ocean

Figure 10 shows an ensemble of more than twenty estimates of the location of the COBs around Pakistan, India, Sri Lanka and Bangladesh (Naini and Talwani, 1982; Powell et al., 1988; Rao et al., 1997; Malod, 1997; Todal and Eldholm, 1998; Calvès et al., 2008; Sreejith et al., 2008; Subrahmanyam et al., 2008; Bouysse et al., 2009; Krishna et al., 2009; Veevers, 2009; Bastia et al., 2010; Corfield et al., 2010; Sinha et al., 2010; Calvès et al., 2011; Arora, 2012; Seton et al., 2012; Gibbons et al., 2013; Rao and Radhakrishna, 2014; Minshull et al.,

2015; Ramana et al., 2015). In addition, at the eastern continental margin of India we show Nemčok et al's (2013) outline of a 20—100 km wide area in which they interpret lower continental crustal slivers and isolated blocks of upper crustal rocks to lie beneath and between ribbons of exhumed mantle lithosphere and volcanic and sedimentary complexes. Although they termed this area 'proto-oceanic crust', the criteria for its interpretation are the same as those for a COTZ.

The COB ensemble on the western margin of India is consistently very large (mean and standard deviation of 475 km and 90 km; Table 1). The maximum width is nearly 670 km. This stems from disagreement about the type of crust under the Laxmi Basin, which lies between the Laxmi Microcontinent and the continental margin around Mumbai (Bhattacharya et al., 1994; Miles et al., 1998). This situation arises from the margin's participation in at least two phases of rifting since Cretaceous times, and its modification by excess volcanism related to the passage of the Deccan-Réunion plume along its underside in Cretaceous and Paleogene times (Collier et al., 2008; Duncan & Hargraves, 1990). On the eastern side of the subcontinent, the mean ensemble uncertainty is smaller, at 184 km, and with a standard deviation of 79 km, measured on 16 equally-spaced profiles (Table 1). Here, the COB estimate of Krishna et al. (2009) transects the ensemble, being second most distal in the NE, and second most proximal in the south. Nemčok et al.'s (2013) COTZ or 'proto-oceanic crust' for this margin is somewhat narrower than the ensemble width, at close to 100 km, and largely enclosed by it.

North Atlantic

The ensemble of North Atlantic COB and COTZ location estimates in Figure 11 consists of more than forty members (Dunbar and Sawyer, 1985; Boillot and Winterer, 1988; Todd et al., 1988; Roest and Srivastava, 1989; Eldholm, 1991; Faleide et al., 1991; Vorren et al., 1991; Pinheiro et al., 1992; Skogseid et al., 1992; Keen and Dehler, 1993; Escher and Pulvertaft, 1995; Whittaker et al., 1997; Breivik et al., 1999; Scott, 2000; Srivastava et al., 2000; Holbrook, 2001; Mosar et al., 2002; Tsikalas et al., 2002; Thinon et al., 2003; Kimbell et al., 2005; Lundin and Doré, 2005; Naylor and Shannon, 2005; Engen et al., 2006; Maillard et al., 2006; Skaarup et al., 2006; Tucholke et al., 2007; Voss and Jokat, 2007; Engen et al., 2008; Mjelde et al., 2008; Bouysse et al., 2009; Gaina et al., 2009; Voss et al., 2009; Peron-Pinvidic

and Manatschal, 2010; Libak et al., 2012; Oakey et al, 2012; Peron-Pinvidic et al., 2012; Seton et al., 2012; Suckro et al., 2012; Hosseinpour et al., 2013; Gernigon et al., 2015; Tasrianto and Escalona, 2015). Like those for the Australian-Antarctic margins, this ensemble includes significant lengths of sheared margin segments, bordering Fram Strait, in which COB locational uncertainty is smaller than 100 km. Away from this, the East Greenland and Newfoundland COB estimates spread over a mean width of 136 km. The population's standard deviation is 94 km (Table 1). The COBs that have been estimated for the conjugates to these margins, off northern and western Europe, show a mean ensemble width of 135 km, and standard deviation of 120 km (Table 1). In Davis Strait and the Labrador Sea, the mean and standard deviations of the COB ensemble's width are 149 km and 84 km. Considering all of the margins together, the largest COB uncertainties are characteristic of the most-frequently estimated COB segments, as was the case in the South China Sea.

Figure 11 also shows a number of separate COTZs, four of which overlap on part of the eastern margin of Greenland. Escher and Pulvertaft's (1995) COTZ is around 30 km wide off east Greenland where it overlaps with the proximal portion of the 150 km wide COTZ of Peron-Pinvidic and Manatschal (2010). This second COTZ estimate is one of a set that is consistently very wide (e.g. up to 300 km off the British Isles). It is difficult to compare these estimates to the ensemble meaningfully, however, because Peron-Pinvidic and Manatschal's (2010) definition of the COTZ includes what they refer to as thinned yet undoubtedly continental crust. As off western India, the widest sections of these COTZs include features that have alternatively been interpreted as microcontinents. Excepting Peron-Pinvidic and Manatschal's (2010) COTZs, the COTZ interpretations tend to be narrower than the COB ensemble (for example off NE Greenland or the southern margin of the Labrador Sea). Off SE Greenland, not only are two of the COTZ interpretations narrower than the COB ensemble, they also map partly or completely outside of it, and exclusively of one another. Alongside the observation that the COB ensembles routinely exceed the published COTZ estimates in width, this illustrates starkly that COTZs are as much subject to interpretational biases as COBs are.

South Atlantic

Gaina et al. (2013) reviewed published estimates of profile-based COTZ widths for the African margin of the South Atlantic, concluding that individual COTZs on different parts of the margin vary in width over a range of 100-150 km. Our ensemble of 23 South Atlantic COBs is shown in Figure 12 (Rabinowitz and LaBrecque, 1979; Raillard, 1990; Nürnberg and Müller, 1991; Chang et al., 1992; Light et al., 1993; Gladczenko et al., 1997; Lawver et al., 1998; Cainelli and Mohriak, 1999; Karner and Driscoll, 1999; Bauer et al., 2000; Macdonald et al., 2003; König and Jokat, 2006; Blaich et al., 2008; Torsvik et al., 2009; ; Pawlowski, 2009; Bouysse et al., 2009; Anka, 2010; Labails et al., 2010; Peyve, 2010; Seton et al., 2012; Gaina et al., 2013; Heine et al., 2013; Wildman et al., 2015). Although this is the largest of the regions shown, and has the longest publication history for COB estimates, the relatively small ensemble reflects the long-standing frontier status of the continental margins of Africa and South America in the exploration industry. Of the margin segments shown, the ensemble-based uncertainties for the COBs are smallest in the equatorial (sheared) segment of the west African margin, at about 60-80 km, and largest in the Santos and Campos basins off Brazil.

Excluding the sheared equatorial segments, the ensemble mean width is 167 km on the west African margin, with a standard deviation of 62 km (Table 1; measured on 21 equally spaced profiles across parts of the margin with at least three COB estimates). On its South American conjugate, the mean width of the ensemble is 217 km and the standard deviation is 194 km (23 profiles; Table 1). The difference between the two ensembles is largely attributable to the extraordinary variety of COB estimates for the Santos Basin segment of the South American margin, whose locations according to different authors disagree in places by more than 800 km. The estimates transect one another strongly. At the southern limits of the South Atlantic, the COB estimate of Nürnberg and Müller (1991) is the most distal of the ensembles on both continental margins, whilst it is one of the most proximal COB estimates in the northern part of the South Atlantic. In part at least, this is likely to reflect the plate kinematic focus of Nürnberg and Müller's study. South Atlantic opening was markedly asynchronous, occurring around 40 Myr earlier in the south than in the north (Eagles, 2007; Pérez-Díaz and Eagles, 2014). Reconstructing the continents under these constraints, whilst trying to avoid deforming them internally by large amounts, requires an interpretation of more distal COBs in the south than in the north.

Discussion

The ensembles consistently show a mean uncertainty (globally, 167 km) that eclipses the expected observational uncertainty for COB identification criteria, as well as a broad standard deviation (globally, 120 km) in estimated COB locations (Table 1). Figure 13 demonstrates that the uniformly large uncertainty in COB location estimates is not a consequence of the challenge of consistently interpreting COBs from data of varying vintages and qualities. Sixty per cent of the COB estimates in our ensembles were published over the last decade, whereas eighty per cent of the 'extreme' widths of the ensembles are products of the publication of pairs of new COB estimates during that period. Table 1 also shows that the globally large uncertainty is not a result of large differences in the ease of COB estimation at either magma rich or magma poor margins, as mapped by Boillot and Coulon (1998). Neither of the uncertainties in estimated COB locations for these magma-availability ensembles significantly differs from the large global mean value, although it should be noted the statistics for magma rich margins are affected by the broad range of opinions regarding the location of the COB west of India. Nonetheless, even if this particular margin were disregarded, the mean COB locational uncertainty for magma rich margins would still be significantly greater than the expected observational uncertainty, at 134 km. The 41 km difference between this value and that for magma poor margins may not be significant, as it lies within the range of observational uncertainties given earlier. For this reason, together with the quite arbitrary decision to disregard the western Indian ensemble in the first place, we consider it would be inappropriate to interpret the uncertainties of COB locations at magma rich and magma poor margins in terms of process.

What is clear though is that the uncertainties of COB location estimates are large and independent of data quality, geographic location, or melt availability at extended margins worldwide. These figures and observations belie any sense that the uncertainty in COB locations might be chiefly observational in origin. COB location is instead clearly dominated by interpreter choice. The widths of our COB ensembles also consistently exceed those of single-study COTZ estimates at both magma-rich and magma-poor margins. We conclude on this basis that published COTZ widths are also strongly influenced by interpreter choice. This should come as little surprise when we recall, as outlined in previous sections, that the

classification of COTZs on the basis of melt availability implies changes of emphasis in interpretations of magmatic and fault-related features, but that both classes of features can just as well be expected to result from the creation of oceanic crust. Given their basis in work by a global community of interpreters using what we would expect to be the full range of currently-plausible interpretations of breakup processes, it should be appropriate to use our COB ensembles as a conservative global set of COTZ estimates. Next, we discuss the consequences of our conclusions for two of the tasks that COBs have previously been routinely used in.

Consequences of COB locational uncertainty for palinspastic reconstructions

One of the main tasks that COBs are used in is palinspastic reconstruction. The task involves restoring the innermost edge of the oceanic crust towards the continental margin by undoing the spatial effects of processes involved in COTZ formation. Some studies refer to the COB, when used for this purpose, as LaLOC or LOC ((Landward) Limit of Oceanic Crust; Heine et al., 2013; Christeson et al., 2014). Its modelled pre-stretching equivalent has been referred to as the restored COB; Williams et al., 2011). As for the COB, mapping or modelling LaLOC or restored COB depends on interpretations and assumptions that balance multiple geophysical observations with predictions or expectations coming from models of continental divergence and failure. The effects of all these assumptions and interpretations on the reliability and accuracy of palinspastic restorations are not clearly understood. As outlined above, after assuming the accuracy of restored COBs to be poor, some studies have suggested that an alternative, and equally valid, alternative to palinspastic modelling is to assume the existence of some observable proxy for the restored COB (Lawver et al., 1998; Macdonald et al., 2003). Macdonald et al. (2003) identify one such proxy at the shelf-edge related free-air gravity anomaly, and they refer to it as the Pre-Breakup Ocean Continent Boundary. They note that this proxy is not reliable at margin segments where the shelf has undergone long-distance progradation, such as beneath the Niger Delta. As discussed above, the observational uncertainty in this gravity anomaly is in the region of 100—150 km.

The aim of palinspastic modelling is to undo the changes in shape of mapped features that have occurred as a consequence of crustal extension. After some take into account the

effects of igneous crustal addition, all palinspastic modelling procedures assume that present-day crustal thickness variability is a consequence of the crustal extension that occurs in plate divergence. In its simplest form, this may involve determining the cross sectional area of extended continental crust imaged by a seismic profile and balancing this with the area in a shorter profile with crust of some assumed pre-extensional thickness (e.g. Heine et al., 2013). Working similarly, but in three dimensions, a set of plate rotation parameters can be assumed as known in order to define profiles along which to exactly balance the crustal thickness sampled from a grid (e.g. Dunbar and Sawyer, 1989). Alternatively, the process may involve searching for a set of plate kinematic rotations that achieve the closest to uniform pre-stretching crustal thickness in a grid (e.g. Grobys et al., 2008). Heine et al. (2013) balanced a set of crustal scale seismic profiles across the South Atlantic margins using an ensemble of COB estimates with a smaller uncertainty (20—135 km) than that in Figure 12. Using crustal thickness grids and gravity-based models of crustal thickness and igneous addition, Williams et al. (2011), Hosseinpour et al. (2013) and Bai et al. (2015) presented palinspastic reconstructions using multiple COB estimates at the conjugate margins in the Labrador Sea and SE Indian oceans, again with somewhat smaller uncertainty than our ensembles imply. All of these studies showed that the choice of post-stretching COB location had only a modest influence on its palinspastically-restored equivalent. This is because any differences between COB location estimates will be reduced by the COTZ's lengthening factor in the corresponding restored COB separations. As lengthening factors on extended continental margins are expected to approach and exceed 4, this effect is great enough that the uncertainty implied by restoration of an ensemble of COBs like any of those in Table 1 would be something like the observational component of uncertainty in any of the ensemble's members (~10—100 km), or somewhat less than the statistical uncertainty of points rotating about the stage poles that are taken to describe rift-stage plate divergence in plate kinematic reconstructions (Figure 14). What is more, within this range of uncertainty, the restored COBs tend to cluster at the continental slope gravity anomalies at extended margins (Figure 13; Heine et al., 2013; Hosseinpour et al., 2013; Williams et al., 2011). This supports Lawver et al.'s (1998) and Macdonald et al.'s (2003) assertions that the slope anomalies, or indeed the continental slope itself, are serviceable proxies for the extent of continental crust prior to stretching. With this in mind, future work on adding to COB ensembles with current interpretation tools and methods

would be unlikely to improve the quality of palinspastic models at extended continental margins. Instead, the continental slope gravity anomaly can serve as an adequate and model-independent alternative to restored COBs.

Consequences of COB locational uncertainty for plate kinematic modelling

The insignificance of the COB in terms of process, the insensitivity of palinspastic reconstructions to interpretational variety in the range of COB estimates, the widespread coincidence of restored COB locations with the continental slope gravity anomaly, and the significant uncertainty in COB dating (~5 Myr for point estimates on linear COBs) compared to the suggested durations of COTZ formation (~10 Myr; Whitmarsh et al., 2001) brings into question the need for precise COB estimates of the kinds presented in our ensembles. However, precise COBs are sometimes made to play a role in tectonic and paleogeographic reconstructions that is rather more sensitive to their location and uncertainty than palinspastic modelling is. That role is in the determination of Euler rotations by which a pair of plates can be estimated to have moved relative to one another over a period of time. Recent studies by Moulin et al. (2009), Blaich et al. (2008), Torsvik et al. (2009), Williams et al. (2011), Ball et al. (2013), Gaina et al. (2013), and Gibbons et al. (2013), all state that they use COB markers to determine or test rotation parameters for plate reconstructions, by searching for rotations that unite them. Some do this by choosing a pair of preferred COB estimates for modelling as conjugates to generate rotations for the time of seafloor spreading onset. Others search for rotations to fit single or multiple palinspastically restored COB estimates in order to reconstruct for the time prior to continental extension. All assume that the COBs chosen for modelling are precisely locatable conjugates, and that they are precisely dateable isochrons.

We have seen that neither of these assumptions seems to be valid. The fact that many of the COBs in the ensembles transect the others suggests that strike is not an attribute of COBs that is easily or consistently estimated. Unfortunately, strike is the parameter of reconstruction figures to which the process of estimating plate rotations is most sensitive. This makes rotation schemes built using single pairs of COBs prone to large errors, and thus great uncertainty. Just as seriously, as we have seen, the age of the COB is in many places not attributable at much better than 5 Myr resolution. As an illustration of the ambiguity

these problems can lead to, Figure 15 shows some of the consequences of using COB estimates for generating and testing plate kinematic reconstructions. In it, the ensemble of South American margin COBs is rotated towards its African counterpart using three separate rotation schemes. The ensembles have not been palinspastically reconstructed, and so the reconstructions depict the South Atlantic margins at the onset of seafloor spreading.

The first scheme uses a single rotation that we have sought to fit the ensembles together for visual satisfaction, assuming their entire lengths represent conjugate isochrons. A large area of overlap centres on the Santos and Campos basins, where we have seen the COB estimates to diverge most widely of any extended continental margin segment in the world. The reconstruction rotation is about a pole at 31.3°W, 43.8°N. This pole is just 60 km distant from the pole determined for full reconstruction of the South Atlantic by Bullard et al (1965), using the 200 fathom (~400 m) submarine contour as a proxy for the sundered edges of the South American and African continents. This reinforces the conclusion that there is little to be gained from investing more effort in new interpretations of COB locations over simply adopting the continental slope or related gravity anomaly in areas where long-distance shelf progradation can be ruled out.

The second reconstruction in Figure 15 uses the South Atlantic pre-opening rotations of Torsvik et al. (2009), which are based on fitting those authors' own estimated COBs together, along with an allowance for intracontinental and extensional margin deformation during the opening of the South Atlantic that the authors adopted from earlier plate kinematic work by Nürnberg and Müller (1991). Practically, this means that Torsvik and his co-authors did not explicitly treat their entire COBs as isochrons. Instead, they divided their COBs into three segments with implied ages of ~150 Ma, 129 Ma, and 112 Ma, from south to north. As in the rigid case, the plate kinematic model causes the COB estimate ensembles to overlap significantly more in the Santos Basin than elsewhere, where the COB ensembles overlap by amounts that, visually at least, are similar to their starting widths.

The third reconstruction uses rotations generated on the basis of seafloor spreading data alone, without leading constraints from COB shapes, by Pérez-Díaz and Eagles (2014),

although those authors did use short segments of shelf edge gravity anomalies as a kind of buffer to constrain maximum angles for some of their rotations. In this reconstruction, the COB ensembles have been broken into seven short conceptually-isochronous segments that enable the kinematic model to optimize their fit by rotating them for seven separate ages. The segmentation of the COB ensembles in Figure 15 resembles that in the reconstructions of Eagles (2007), which were based on consideration of the coarse-resolution ages of breakup unconformities and breakup-related volcanism. Like the others, this reconstruction features a large overlap in the Santos Basin segment but is otherwise visually acceptable.

The misfit values calculated for the three reconstructions in Figure 15 are all quite similar, although no numerical attempt has been made to minimize them. From the values shown, it should come as no surprise that the smallest misfit was achieved using the greatest flexibility in COB segmentation and age. Recalling, however, that there are no explicit constraints on COB age and that the proxy ages applied to them are likely to be both imprecise and inaccurate, it is clear that there is little we know with confidence about the COB ensembles that might lead us to prefer any of the three models as a starting point for minimizing the misfit. Instead, we conclude that once the uncertainty in its interpretation and location is taken into consideration, there can be little confidence in the COB's suitability as a tool for testing plate kinematic hypotheses by the generation of rotations or reconstructions from fitting them.

Summary

There is no unique diagnostic process by which COBs are known to form, and therefore no sharp definition of the COB that might be used to map it. Locating COBs is a matter of observation in geophysical data, which involves errors on the order of 10—100 km, and of interpretation of the observations in the light of models or concepts of continental breakup processes. Ensembles of COB estimates show that this interpretational step introduces an additional component of error that increases the total uncertainty in any given COB location estimate by up to a few hundred kilometres. COB ages are not directly determined, but may be assigned with up-to multi-million year uncertainty on the basis of considerations of proxy features at continental margins.

When making palinspastic reconstructions of COB ensembles at extended continental margins, the large overall uncertainty in the post-stretching location of the COB reduces to a value close to or less than that uncertainty's lesser, observational, component. The choice of COB is thus not of great significance to the palinspastic reconstruction process. The results of using estimated COBs for plate kinematic modelling are strongly dependent on their segmentation and assignment to conjugate pairs, dating, and their estimated strike. None of these qualities is tightly constrainable within the uncertainties discussed here, and using COB estimates for plate kinematic modelling can therefore lead to very much larger differences between models than appear between models built using more tightly-constrainable and easily-interpretable features. Whilst a carefully-chosen plate kinematic model may therefore provide a useful context in which to conduct continental breakup studies, such a choice cannot be made on the basis of a plate kinematic model built using COB locations as geometric markers.

Acknowledgements

We thank the COMPASS consortium and Fault Dynamics Research Group at Royal Holloway, and the Alfred Wegener Institute, Helmholtz Centre for Polar and Marine Research, for funding. We thank Bernie Coakley of University of Alaska, Fairbanks, for discussions on this topic, and for reading and commenting on the manuscript. Pete Burgess, RHUL, provided guidance on the theme of breakup unconformities. Tanja Fromm and Tabea Altenbernd, AWI, helped with understanding the interpretation of COBs in seismic refraction profiles.

References

1. Altenbernd, T., Jokat, W., Heyde, I. and Damm, V., 2014, A crustal model for northern Melville Bay, Baffin Bay, J. Geophys. Res., 119, 8610–8632, doi:10.1002/2014JB011559
2. Anka, Z., Seranne, M., and di Primio, R., 2010, Evidence of a large upper-Cretaceous depocentre across the Continent-Ocean boundary of the Congo-Angola basin: Implications for palaeo-drainage and potential ultra-deep source rocks, Marine and Petroleum Geology, 27, 601-611.
3. Arora, K., Tiwari, V.M., Singh, B., Mishra, D.C., and Grevemeyer, I., 2012, Three dimensional lithospheric structure of the western continental margin of India constrained from gravity modelling: implication for tectonic evolution, Geophysical Journal International, 190, 131-150.
4. Bai, Y., Wu, S., Liu, Z., Müller, R.D., Williams, S.E., Zahirovic, S., and Dong, D., 2015, Full-fit reconstruction of the South China Sea conjugate margins, *Tectonophysics*, accepted manuscript, doi:10.1016/j.tecto.2015.08.028

5. Ball, P., G. Eagles, C. Ebinger, K. McClay, and T. Totterdell, 2013, The spatial and temporal evolution of strain during the separation of Australia and Antarctica, Geochem. Geophys. Geosyst., 14, 2771–2799, doi:10.1002/ggge.20160.
6. Barckhausen, U., Engels, M., Franke, D., Ladage, S., & Pubellier, M., 2014, Evolution of the South China Sea: Revised ages for breakup and seafloor spreading, Marine and Petroleum Geology, 58, 599-611.
7. Bastia, R., Radhakrishna, M., Srinivas, T., Nayak, S., Nathaniel, D.M., and Biswal, T.K., 2010, Structural and tectonic interpretation of geophysical data along the eastern continental margin of India with special reference to the deep water petroliferous basins, Journal of Asian Earth Sciences, 39, 608—619, doi:10.1016/j.jseaes.2010.04.031
8. Bastow, I.D., Stuart G.W., Kendall J.-M., and Ebinger C.J., 2005, Upper-mantle seismic structure in a region of incipient continental breakup: northern Ethiopian rift, Geophysical Journal International, 162, 479-493, doi: 10.1111/j.1365-246X.2005.02666.x
9. Bauer, K., Neben, S., Schreckenberger, B., Emmermann, R., Hinz, K., Fechner, N., Gohl, K., Schulze, A., Trumbull, R.B., and Weber, K., 2000, Deep structure of the Namibia continental margin as derived from integrated geophysical studies, J. geophys. Res., 105, 25 829–25 853.
10. Bhattacharya, G.C., Chaubey, A.K., Murty, G.P.S., Srinivas, K., Sarma, K., Subrahmanyam, V. & Krishna, K.S., 1994, Evidence for sea-floor spreading in the Laxmi Basin, northeastern Arabian Sea, Earth planet. Sci. Lett., 125, 211–220.
11. Bird, D.E., Burke, K., Hall, S.A., and Casey, J.F., 2005, Gulf of Mexico tectonic history: Hotspot tracks, crustal boundaries, and early salt distribution, AAPG Bulletin, 89, 311-328.
12. Blaich, O. A., F. Tsikalas, and J. I. Faleide, 2008, Northeastern Brazilian margin: Regional tectonic evolution based on integrated analysis of seismic reflection and potential field data and modeling, Tectonophysics, 458, 51–67, doi:10.1016/j.tecto.2008.02.011.
13. Blaich, O. A., J. I. Faleide, F. Tsikalas, R. Lilletveit, D. Chiossi, P. Brockbank, and P. Cobbold, 2010, Structural architecture and nature of the continent- ocean transitional domain at the Camamu and Almada Basins (northeastern Brazil) within a conjugate margin setting, in Petroleum Geology: From Mature Basins to New Frontiers-Proceedings of the 7th Conference, edited by B. A. Vining and S. C. Pickering, p. 1–17, Geol. Soc., London, doi:10.1144/070000.
14. Blaich, O.A., Faleide, J.I., and Tsikalas, F., 2011, Crustal breakup and continent-ocean transition at South Atlantic conjugate margins, Journal of Geophysical Research, 116, B01402, doi:10.1029/2010JB007686
15. Boillot, G., Winterer, E.L., Meyer, A.W., et al., 1987. Proc. ODP, Init. Repts., 103: College Station, TX (Ocean Drilling Program). doi:10.2973/odp.proc.ir.103.1987
16. Boillot, G., Winterer, E., 1988. Drilling on the Galicia margin: retrospect and prospect. Proceedings of the Ocean Drilling Program, Scientific Results, 103, 809–828.
17. Boillot, G., and Froitzheim, N., 2001, Non-volcanic rifted margins, continental break-up and the onset of sea-floor spreading: some outstanding questions. Geological Society, London, Special Publications, 187, 9-30.
18. Boillot, G. and Coulon, C., 1998, La déchirure continentale et l'ouverture océanique. Gordon and Breach Science publishers, Amsterdam, p 208
19. Bosworth, W., & Burke, K., 2005, Evolution of the Red Sea—Gulf of Aden rift system. *Petroleum systems of divergent continental margin basins*, 342-372.
20. Bouysse, P., et al., 2009, Geological Map of the World at 1:25 M (3rd edition), 2 sheets, CGMW 2009.
21. Breivik, A.J., Verhoef, J. and Faleide, J.I., 1999, Effect of thermal contrasts on gravity modeling at passive margins: Results from the western Barents Sea. Journal of Geophysical Research, 104, 15293-15311, doi: 10.1029/1998JB900022.
22. Briais, A., P. Patriat, and Tapponnier, P., 1993, Updated interpretation of magnetic anomalies and seafloor spreading stages in the south China Sea: Implications for the Tertiary tectonics of Southeast Asia, J. Geophys. Res., 98, 6299–6328, doi:10.1029/92JB02280.
23. Bridges, D.L., Mickus, K., Gao, S.S., Abdelsalam, M.G. & Alemu, A., 2012. Magnetic stripes of a transitional continental rift in Afar, Geology, 40, 203–206.
24. Brown, B.J., Müller, R.D., Gaina, C., Struckmeyer, H.I.M., Stagg, H.M.J., and Symonds, P.A., 2003, Formation and evolution of Australian passive margins: implications for locating the boundary between continental and oceanic crust, GSA Special Paper, 372, 223-243.
25. Buffler, R. T., and D. S. Sawyer, 1985, Distribution of crust and early history, Gulf of Mexico Basin: Gulf Coast Association of Geological Societies Transactions, 35, 333–334.
26. Buffler, R. T., and W. A. Thomas, 1994, Crustal structure and evolution of the southeastern margin of

North America and the Gulf of Mexico, in R. C. Speed, ed., Phanerozoic evolution of North American continent-ocean transitions: Boulder, Geological Society of America, The Decade of North American Geology Summary Volume, p. 219–264.

27. Bullard, E., J. E. Everett, and A. G. Smith, 1965, The fit of the continents around the Atlantic, Philos. Trans. R. Soc. London A: Mathematical, Physical and Engineering Sciences, 258, 41–51.
28. Burgess, P. M., & Hovius, N., 1998, Rates of delta progradation during highstands: consequences for timing of deposition in deep-marine systems, Journal of the Geological Society, 155, 217-222.
29. Calvès, G., P. D. Clift, and A. Inam (2008), Anomalous subsidence on the rifted volcanic margin of Pakistan: No influence from Deccan plume, Earth Planet. Sci. Lett., 272, 231–239, doi:10.1016/j.epsl.2008.04.042.
30. Calvès, G., Schwab, A.M., Huuse, M., Clift, P.D., Gaina, C., Jolley, D., Tabrez, A.R. & Inam, A., 2011. Seismic volcanostratigraphy of the western Indian rifted margin: the pre-Deccan igneous province, J. geophys. Res., 116, B01101, doi:10.1029/2010JB000862.
31. Cainelli, C., and Mohriak, W.U., 1999, Some remarks on the evolution of sedimentary basins along the Eastern Brazilian continental margin, Episodes, 22, 206–216.
32. Cameselle, A.L., Ranero, C.R., Franke, D., and Barckhausen, U., 2015, The continent-ocean transition on the norhtwestern South China Sea, Basin Research, 1-23, doi:10.1111/bre.12137
33. Canales, J. P., Nedimović, M. R., Kent, G. M., Carbotte, S. M., & Detrick, R. S., 2009, Seismic reflection images of a near-axis melt sill within the lower crust at the Juan de Fuca ridge. Nature, 460, 89-93.
34. Chang, H. K., Kowsmann, R. O., Figueiredo, A. M. F., & Bender, A., 1992, Tectonics and stratigraphy of the East Brazil Rift system: an overview. Tectonophysics, 213, 97-138.
35. Chen, L., 2014, Stretching factor estimation for the long-duration and multi-stage continental extensional tectonics: Application to the Baiyun Sag in the northern margin of the South China Sea, Tectonophysics, 611, 167-180, doi:10.1016/j.tecto.2013.11.026
36. Christensen, N. I., & Mooney, W. D., 1995, Seismic velocity structure and composition of the continental crust: A global view. Journal of Geophysical Research, 100, 9761-9788.
37. Christeson, G. L., H. J. A. Van Avendonk, I. O. Norton, J. W. Snedden, D. R. Eddy, G. D. Karner, and C. A. Johnson, 2014, Deep crustal structure in the eastern Gulf of Mexico, J. Geophys. Res., 119, 6782–6801, doi:10.1002/2014JB011045.
38. Close, D. I., A. Watts, and H. Stagg, 2009, A marine geophysical study of the Wilkes Land rifted continental margin, Antarctica, Geophys. J. Int., 177, 430–450.
39. Collier, J.S., Sansom, V., Ishizuka, O., Taylor, R.N., Minshull, T.A. & Whitmarsh, R.B., 2008. Age of Seychelles–India break-up, Earth planet. Sci. Lett., 272, 264–277.
40. Corfield, R.I., Carmichael, S., Bennett, J., Akhter, S., Fatimi, M. & Craig, T., 2010. Variability in the crustal structure of the West Indian Continental Margin in the Northern Arabian Sea, Petrol. Geosci., 16, 257–265.
41. Del Ben, A., and Mallardi, A., 2004, Interpretation and chronostratigraphic mapping of multichannel seismic reflection profile I95167, Eastern Falkland Plateau (South Atlantic), Marine geology, 209, 347-361.
42. Deng, J. M., Wang, T. K., Yang, B. J., Lee, C. S., Liu, C. S., & Chen, S. C., 2012, Crustal velocity structure off SW Taiwan in the northernmost South China Sea imaged from TAIGER OBS and MCS data. Marine Geophysical Research, 33, 327-349.
43. Dick, H. J., Lin, J., & Schouten, H., 2003, An ultraslow-spreading class of ocean ridge. Nature, 426, 405-412.
44. Direen, N. G., Stagg, H. M., Symonds, P. A., & Colwell, J. B., 2011, Dominant symmetry of a conjugate southern Australian and East Antarctic magma-poor rifted margin segment. Geochemistry, Geophysics, Geosystems, 12, Q02006, doi:10.1029/2010GC003306.
45. Drake, C. L., and Kosminskaya, I. P., 1969, The transition from continental to oceanic crust, Tectonophysics, 7, 363-384.
46. Dunbar, J. A., & Sawyer, D.S., 1989, How preexisting weaknesses control the style of continental breakup. Journal of Geophysical Research, 94, 7278-7292.
47. Duncan,R.A. & Hargraves, R.B., 1990, $^{40}Ar/^{39}Ar$ geochronology of basement rocks from the Mascarene Plateau, the Chagos Bank, and the Maldives Ridge, in Proceedings of the ODP, Sci. Results, 115, 43–51, eds Duncan, R.A. et al., College Station, TX (Ocean Drilling Program).
48. Eagles, G., 2004, Tectonic evolution of the Antarctic—Phoenix plate system since 15 Ma, Earth and Planetary Science Letters, 217, 97—109, doi:10.1016/S0012-821X(03)00584-3

49. Eagles, G., 2007, New angles on South Atlantic opening. Geophysical Journal International, 168, 353-361.
50. Eagles, G., & König, M., 2008, A model of plate kinematics in Gondwana breakup. Geophysical Journal International, 173, 703-717.
51. Eagles, G., Gloaguen, R., & Ebinger, C., 2002, Kinematics of the Danakil microplate, Earth and Planetary Science Letters, 203, 607-620.
52. Eittreim, S. L., 1994, Transition from continental to oceanic crust on the Wilkes-Adelie margin of Antarctica, J. Geophys. Res., 99, 24189–24205, doi:10.1029/94JB01903.
53. Eldholm, O., & Grue, K., 1994, North Atlantic volcanic margins: dimensions and production rates. Journal of Geophysical Research, 99, 2955-2968.
54. Eldholm, O., 1991, Magmatic evolution of a volcanic rifted margin, Marine Geology, 102, 43-61, doi: 10.1016/0025-3227(91)90005-O
55. Engen, Ø., Faleide, J. I., & Dyreng, T. K., 2008, Opening of the Fram Strait gateway: a review of plate tectonic constraints. Tectonophysics, 450, 51-69.
56. Engen, Ø., Frazer, L. N., Wessel, P., & Faleide, J. I., 2006, Prediction of sediment thickness in the Norwegian–Greenland Sea from gravity inversion. Journal of Geophysical Research, 111, B11403, doi:10.1029/2005JB003924.
57. Escher, J. C., & Pulvertaft, T. C. R., 1995, Geological map of Greenland: Copenhagen. Geological Survey of Greenland, scale, 1(2,500,000).
58. Exon, N. F., Royer, J. Y., & Hill, P. J., 1996, Tasmante cruise: swath-mapping and underway geophysics south and west of Tasmania. Marine Geophysical Researches, 18, 275-287.
59. Faleide, J. I., Gudlaugsson, S. T., Eldholm, O., Myhre, A. M., & Jackson, H. R., 1991, Deep seismic transects across the sheared western Barents Sea-Svalbard continental margin. Tectonophysics, 189, 73-89.
60. Falvey, D.A., 1974. The development of continental margins in plate tectonic theory. Australian Petroleum Exploration Association Journal 14, 95-107.
61. Franke, D., Neben, S., Schreckenberger, B., Schulze, A., Stiller, M., & Krawczyk, C. M., 2006, Crustal structure across the Colorado Basin, offshore Argentina. Geophysical Journal International, 165, 850-864.
62. Fromm, T., Planert, L., Jokat, W., Ryberg, T., Behrmann, J.H., Weber, M.H., and Haberland, C., 2015, South Atlantic opening: a plume-induced breakup? Geology, in press, doi:10.1130/G36936.1
63. Fullerton, L. G., Sager, W. W., & Handschumacher, D. W., 1989, Late Jurassic-Early Cretaceous evolution of the eastern Indian Ocean adjacent to northwest Australia, Journal of Geophysical Research, 94, 2937-2953.
64. Gaina, C., Gernigon, L., & Ball, P., 2009, Palaeocene–Recent plate boundaries in the NE Atlantic and the formation of the Jan Mayen microcontinent. *Journal of the Geological Society*, *166*, 601-616.
65. Gaina, C., Müller, R. D., Brown, B. J., & Ishihara, T., 2003, Microcontinent formation around Australia. Geological Society of America Special Papers, 372, 405-416.
66. Gaina, C., Müller, R. D., Brown, B., Ishihara, T., & Ivanov, S., 2007, Breakup and early seafloor spreading between India and Antarctica. Geophysical Journal International, 170, 151-169.
67. Gaina, C., Müller, D. R., Royer, J. Y., Stock, J., Hardebeck, J., & Symonds, P., 1998, The tectonic history of the Tasman Sea: a puzzle with 13 pieces. Journal of Geophysical Research, 103, 12413-12433.
68. Gaina, C., Torsvik, T. H., van Hinsbergen, D. J., Medvedev, S., Werner, S. C., & Labails, C., 2013, The African Plate: A history of oceanic crust accretion and subduction since the Jurassic. Tectonophysics, 604, 4-25.
69. Gernigon, L., A. Blischke, A. Nasuti, and M. Sand, 2015, Conjugate volcanic rifted margins, sea-floor spreading and microcontinent: Insights from new high-resolution aeromagnetic surveys in the Norway Basin, Tectonics, 34, doi:10.1002/2014TC003717.
70. Gibbons, A. D., Whittaker, J. M., & Müller, R. D., 2013, The breakup of East Gondwana: Assimilating constraints from Cretaceous ocean basins around India into a best-fit tectonic model, Journal of Geophysical Research, 118, 808-822.
71. Gillard, M., Autin, J., Manatschal, G., Sauter, D., Munschy, M., and Schaming, M., 2015, Tectonomagmatic evolution of the final stages of rifting along the deep conjugate Australian-Antarctic magma-poor rifted margins: Constraints from seismic observations. Tectonics, 34, 753–783. doi: 10.1002/2015TC003850.
72. Gladczenko, T. P., Hinz, K., Eldholm, O., Meyer, H., Neben, S., & Skogseid, J., 1997, South Atlantic volcanic margins. Journal of the Geological Society, 154, 465-470.

73. Gohl, K., 2008, Antarctica's continent–ocean transitions: consequences for tectonic reconstructions. In *Proceedings of the 10th international symposium on Antarctic earth sciences, Polar Research Board, National Research Council, US Geological Survey, The National Academies Press, Washington* (pp. 29-38).
74. Gradstein, F. M., Ogg, J. G., Schmitz, M., & Ogg, G. (Eds.)., 2012, *The Geologic Time Scale 2012 2-Volume Set*, Elsevier.
75. Grobys, J. W. G., K. Gohl, and G. Eagles, 2008, Quantitative tectonic reconstructions of Zealandia based on crustal thickness estimates, Geochem. Geophys. Geosyst., 9, Q01005, doi:10.1029/2007GC001691.
76. Hall, L., Gibbons, A., Bernardel, G., Whittaker, J., Nicholson, C., Rollet, N., Muller, R., 2013, Structural Architecture of Australia's Southwest Continental Margin and Implications for Early Cretaceous Basin Evolution. WABS 2013: West Australian Basins Symposium, Perth, Australia: Petroleum Exploration Society of Australia Limited.
77. Hall, S. A., & Najmuddin, I. J., 1994, Constraints on the tectonic development of the eastern Gulf of Mexico provided by magnetic anomaly data. Journal of Geophysical Research, 99, 7161-7175.
78. Hammond, J.O.S., Kendall, J.-M., Stuart, G.W., Keir, D., Ebinger, C., Ayele, A., and Belachew, M., 2011, The nature of the crust beneath the Afar triple junction: evidence from receiver functions, Geochemistry, Geophysics, Geosystems, 12, Q12004, DOI: 10.1029/2011GC003738
79. Heine, C., & Müller, R. D., 2005, Late Jurassic rifting along the Australian North West Shelf: margin geometry and spreading ridge configuration, Australian Journal of Earth Sciences, 52, 27-39.
80. Heine, C., J. Zoethout, and R. D. Müller, 2013, Kinematics of the South Atlantic rift, Solid Earth Discuss., 5, 41–116, doi:10.5194/sed-5-41-2013.
81. Hellinger, S. J., 1981, The uncertainties of finite rotations in plate tectonics. Journal of Geophysical Research, 86, 9312-9318.
82. Hemant, K., and S. Maus, 2005, Geological modeling of the new CHAMP magnetic anomaly maps using a geographical information system technique, J. Geophys. Res., 110, B12103, doi:10.1029/2005JB003837.
83. Holbrook, W. S., Larsen, H. C., Korenaga, J., Dahl-Jensen, T., Reid, I. D., Kelemen, P. B., Hopper, J.R., Kent, G.M., Lizzaralde, D., Bernstein, S., & Detrick, R. S., 2001, Mantle thermal structure and active upwelling during continental breakup in the North Atlantic. Earth and Planetary Science Letters, 190, 251-266.
84. Holmes, A., 1944, Principles of Physical Geology, Thomas Nelson and Sons.
85. Holmes, A. 1931. Radioactivity and Earth movements. Transactions of the Geological Society of Glasgow for 1928-29, 18, 559-606.
86. Hosseinpour, M., Müller, R. D., Williams, S. E., & Whittaker, J. M. (2013). Full-fit reconstruction of the Labrador Sea and Baffin Bay. Solid Earth, 4, 461-479
87. Hsu, S. K., Yeh, Y. C., Doo, W. B., & Tsai, C. H., 2004, New bathymetry and magnetic lineations identifications in the northernmost South China Sea and their tectonic implications. Marine Geophysical Researches, 25, 29-44.
88. Hu, D., Zhou, D., Wu, X., He, M., Pang, X., & Wang, Y., 2009, Crustal structure and extension from slope to deepsea basin in the northern South China Sea. Journal of Earth Science, 20, 27-37.
89. Hudec, M.R., Norton, I.O., Jackson, M.P.A., and Peel, F.J., 2013, Jurassic evolution of the Gulf of Mexico salt basin, AAPG Bulletin, 97, 1683-1710, doi:10.1306/04011312073
90. Hwang, C., and Chang, E.T.Y., 2014, Seafloor sectrets revealed, Science, 346, 32—33, doi:10.1126/science.1260459
91. Ishihara, T., Leitchenkov, G. L., Golynsky, A. V., Alyavdin, S., & O'Brien, P. E., 1999, Compilation of shipborne magnetic and gravity data images crustal structure of Prydz Bay (East Antarctica), Annals of Geophysics, 42, 229-248
92. Jokat, W., Boebel, T., König, M., & Meyer, U., 2003, Timing and geometry of early Gondwana breakup. Journal of Geophysical Research, 108, 2428, doi:10.1029/2002JB001802, B9.
93. Jokat, W., & Schmidt-Aursch, M. C., 2007, Geophysical characteristics of the ultraslow spreading Gakkel Ridge, Arctic Ocean. Geophysical journal international, 168, 983-998.
94. Karner, G. D., & Driscoll, N. W., 1999, Tectonic and stratigraphic development of the West African and eastern Brazilian Margins: insights from quantitative basin modelling. Geological Society, London, Special Publications, 153, 11-40.
95. Keen, C. E., & Dehler, S. A., 1993, Stretching and subsidence: rifting of conjugate margins in the North Atlantic region. Tectonics, 12, 1209-1229.

96. Kimbell, G. S., Ritchie, J. D., Johnson, H., & Gatliff, R. W., 2005, Controls on the structure and evolution of the NE Atlantic margin revealed by regional potential field imaging and 3D modelling. In *Geological Society, London, Petroleum Geology Conference series* (Vol. 6, pp. 933-945). Geological Society of London.
97. Kirkwood, B.H., Royer, J.Y., Chang, T.C., & Gordon, R.G., 1999, Statistical tools for estimating and combining finite rotations and their uncertainties, Geophysical Journal International, 137, 408-428.
98. König, M., & Jokat, W., 2006, The Mesozoic breakup of the Weddell Sea. Journal of Geophysical Research, 111, B12102, doi:10.1029/2005JB004035.
99. Klingelhöfer, F., Evain, M., Afilhado, A., Rigoti, C., Loureiro, A., Alves, D., Lepretre, A., Moulin, M., Schnurle, P., Benebdellouahed, M., Baltzer, A., Rabineau, M., Feld, A., Viana, A., and Aslanian, D., 2014, Imaging proto-oceanic crust off the Brazilian Continental Margin. Geophysical Journal International, 200, 471-488.
100. Krishna, K. S., Michael, L., Bhattacharyya, R., & Majumdar, T. J., 2009, Geoid and gravity anomaly data of conjugate regions of Bay of Bengal and Enderby Basin: New constraints on breakup and early spreading history between India and Antarctica. Journal of Geophysical Research, 114, B03102, doi:10.1029/2008JB005808.
101. Kyrkjebø, R., Gabrielsen, R. H., & Faleide, J. I., 2004, Unconformities related to the Jurassic–Cretaceous synrift–post-rift transition of the northern North Sea. Journal of the Geological Society, 161, 1-17.
102. Labails, C., Olivet, J.-L., Aslanian, D., and Roest, W.R., 2010, An alternative early opening scenario for the Central Atlantic Ocean, Earth and Planetary Science Letters, 297, 355-368, http://dx.doi.org/10.1016/j.epsl.2010.06.024
103. Laske, G., Masters, G., Ma, Z. and Pasyanos, M., 2013, Update on CRUST1.0 - A 1-degree Global Model of Earth's Crust, Geophys. Res. Abstracts, 15, Abstract EGU 2013-2658.
104. Lawver, L. A., Gahagan, L. M., & Dalziel, I. W., 1998, A tight fit-Early Mesozoic Gondwana, a plate reconstruction perspective. Memoirs of National Institute of Polar Research. Special issue, 53, 214-229.
105. Leitchenkov, G., Guseva, J., Gandyukhin, V., Grikurov, G., Kristoffersen, Y., Sand, M., Golynsky, A., and Aleshkova, N., 2008, Crustal structure and tectonic provinces of the Riiser-Larsen Sea area (East Antarctica): results of geophysical studies. Marine Geophysical Researches, 29, 135-158.
106. Leitchenkov, G. L., Guseva, Y. B., Gandyukhin, V. V., Ivanov, S. V., & Safonova, L. V., 2014, Structure of the Earth's crust and tectonic evolution history of the Southern Indian Ocean (Antarctica). Geotectonics, 48, 5-23.
107. Levi, S., & Riddihough, R., 1986, Why are marine magnetic anomalies suppressed over sedimented spreading centers? Geology, 14, 651-654
108. Li, C., & Song, T., 2012, Magnetic recording of the Cenozoic oceanic crustal accretion and evolution of the South China Sea basin. Chinese Science Bulletin, 57, 3165-3181.
109. Li, C., J. Li, W. Ding, D. Franke, Y. Yao, H. Shi, X. Pang, Y. Cao, J. Lin, D. K. Kulhanek, T. Williams, R. Bao, A. Briais, E. A. Brown, Y. Chen, P. D. Clift, F. S. Colwell, K. A. Dadd, I. Hernández-Almeida, X. Huang, S. Hyun, T. Jiang, A. A. P. Koppers, Q. Li, C. Liu, Q. Liu, Z. Liu, R. H. Nagai, A. Peleo-Alampay, X. Su, Z. Sun, M. L. G. Tejada, H. S. Trinh, Y. Yeh, C. Zhang, F. Zhang, G. Zhang, and X. Zhao, 2015, Seismic stratigraphy of the central South China Sea basin and implications for neotectonics. J. Geophys. Res. Solid Earth, 120, 1377–1399. doi: 10.1002/2014JB011686.
110. Libak, A., Mjelde, R., Keers, H., Faleide, J. I., & Murai, Y., 2012, An integrated geophysical study of Vestbakken Volcanic Province, western Barents Sea continental margin, and adjacent oceanic crust. Marine Geophysical Research, 33, 185-207.
111. Light, M. P. R., Maslanyj, M. P., Greenwood, R. J., & Banks, N. L., 1993, Seismic sequence stratigraphy and tectonics offshore Namibia. Geological Society, London, Special Publications, 71, 163-191.
112. Lister, G.S., Etheridge, M.A., and Symonds, P.A., 1986, Detachment faulting and the evolution of passive continental margins, Geology, 14, 246—250.
113. Lundin, E.R. and Doré, A.G., 2011, Hyperextension, serpentinization, and weakening: A new paradigm for rifted margin compressional deformation, Geology, 39, 347-350, doi: 10.1130/G31499.1
114. Macdonald, D., Gomez-Perez, I., Franzese, J., Spalletti, L., Lawver, L., Gahagan, L., Dalziel, I., Thomas, C.G.C., Trewin, N.H., Hole, M.J. & Paton, D., 2003, Mesozoic break-up of SW Gondwana: implications for regional hydrocarbon potential of the southern South Atlantic. Marine and Petroleum Geology, 20, 287-308.

115. Maillard, A., Malod, J., Thiébot, E., Klingelhoefer, F., & Réhault, J. P., 2006, Imaging a lithospheric detachment at the continent–ocean crustal transition off Morocco. Earth and Planetary Science Letters, 241, 686-698.
116. Malod, J. A., Droz, L., Kemal, B. M., & Patriat, P., 1997, Early spreading and continental to oceanic basement transition beneath the Indus deep-sea fan: northeastern Arabian Sea. Marine geology, 141, 221-235.
117. Manatschal, G., 2004, New models for evolution of magma poor rifted margins based on a review of data and concepts from West Iberia and the Alps. International Journal of Earth Sciences, 93, 432-466.
118. Manatschal, G. and Nievergelt, P. A., 1997, continent-ocean transition recorded in the Err and Platta nappes (Eastern Switzerland). Eclogae Geol. Helvetiae 90, 3–27.
119. Marton, G., and R. T. Buffler, 1994, Jurassic reconstruction of the Gulf of Mexico Basin: International Geology Review, 36, 545–586.
120. Miles, P. R., Munschy, M., & Segoufin, J., 1998, Structure and early evolution of the Arabian Sea and East Somali Basin. Geophysical Journal International, 134, 876-888.
121. Minshull, T.A., Edwards, R.A., and Flueh, E.R., 2015, Crustal structure of the Murray Ridge, northwest Indian Ocean, from wide-angle seismic data, Geophysical Journal International, 202, 454—463, doi:10.1093/gji/ggv162.
122. Mjelde, R., Kodaira, S., Shimamura, H., Kanazawa, T., Shiobara, H., Berg, E. W., & Riise, O., 1997, Crustal structure of the central part of the Vøring Basin, mid-Norway margin, from ocean bottom seismographs. Tectonophysics, 277, 235-257.
123. Moores E. M. and F. J. Vine, 1971, The Troodos massif, Cyprus, and other ophiolites as oceanic crust: Evaluation and implications, Philosophical Transactions of the Royal Society of London, 268A, 443-466.
124. Mosar, J., Lewis, G., & Torsvik, T., 2002, North Atlantic sea-floor spreading rates: implications for the Tertiary development of inversion structures of the Norwegian–Greenland Sea, Journal of the Geological Society, 159, 503-515.
125. Moulin, M., Aslanian, D., & Unternehr, P., 2010, A new starting point for the South and Equatorial Atlantic Ocean. Earth-Science Reviews, 98, 1-37.
126. Muller, M.R., Minshull, T. A., & White, R. S., 1999, Segmentation and melt supply at the Southwest Indian Ridge. Geology, 27, 867-870.
127. Müller, R.D., Sandwell, D. T., Tucholke, B. E., Sclater, J. G., & Shaw, P. R., 1991, Depth to basement and geoid expression of the Kane Fracture Zone: a comparison. Marine geophysical researches, 13, 105-129.
128. Müller, R.D., Goncharov, A., & Kritski, A., 2005, Geophysical evaluation of the enigmatic Bedout basement high, offshore northwestern Australia. Earth and Planetary Science Letters, 237, 264-284.
129. Naini, B.R., & Talwani, M., 1982, Structural framework and the evolutionary history of the continental margin of western India. In Studies in continental margin geology (Vol. 34, pp. 167-191). Am. Assoc. Pet. Geol. Mem.
130. Naylor, D., & Shannon, P. M., 2005, The structural framework of the Irish Atlantic Margin. In *Geological Society, London, Petroleum Geology Conference series* (Vol. 6, pp. 1009-1021). Geological Society of London.
131. Nemčok, M., Sinha, S.T., Stuart, C.J., Welker, C., Choudhuri, M., Sharma, S.P., Misra, A.A., Sinha, N., and Venkatraman, S., 2013, East Indian margin evolution and crustal architecture: integration of deep reflection seismic interpretation and gravity modelling. Geological Society, London, Special Publications, 369, 477-496.
132. Nirrengarten, M., Gernigon, L., & Manatschal, G., 2014, Lower crustal bodies in the Møre volcanic rifted margin: Geophysical determination and geological implications, Tectonophysics, 636, 143-157.
133. Nissen, S. S., Hayes, D. E., Buhl, P., Diebold, J., Bochu, Y., Zeng, W., & Chen, Y., 1995, Deep penetration seismic soundings across the northern margin of the South China Sea. Journal of Geophysical Research, 100, 22407-22433.
134. Nogi, Y., Jokat, W., Kitada, K., & Steinhage, D., 2013, Geological structures inferred from airborne geophysical surveys around Lützow-Holm Bay, East Antarctica. Precambrian Research, 234, 279-287.
135. Norvick, M. S., 2004, Tectonic and stratigraphic history of the Perth Basin. Geoscience Australia Record, 16.
136. Norvick, M.S., Langford, R.P., Rollet, N., Hashimoto, T., Earl, K.L. and Morse, M.P., 2008, New insights into the evolution of the Lord Howe Rise (Capel and Faust basins), offshore eastern Australia, from terrane and geophysical data analysis. In: Blevin, J.E., Bradshaw, B.E. and Uruski, C. (eds),

Eastern Australasian Basins Symposium III: Energy security for the 21st century. Petroleum Exploration Society of Australia Special Publication, 291–310.
137. Nürnberg, D., & Müller, R. D., 1991, The tectonic evolution of the South Atlantic from Late Jurassic to present. Tectonophysics, 191, 27-53.
138. Oakey, G. N., & Chalmers, J. A., 2012, A new model for the Paleogene motion of Greenland relative to North America: plate reconstructions of the Davis Strait and Nares Strait regions between Canada and Greenland. Journal of Geophysical Research, 117, B10401, doi: 10.1029/2011JB008942
139. Pawlowski, R., 2008, The use of gravity anomaly data for offshore continental margin demarcation. The Leading Edge, 27, 722-727.
140. Peate, D. W., 1997, The Paraná-Etendeka Province, in Large Igneous Provinces: Continental, Oceanic, and Planetary Flood Volcanism (eds J. J. Mahoney and M. F. Coffin), American Geophysical Union, Washington, D. C.. doi: 10.1029/GM100p0217, p.217-245.
141. Pérez-Díaz, L., & Eagles, G., 2014, Constraining South Atlantic growth with seafloor spreading data. Tectonics, 33, 1848-1873.
142. Peron-Pinvidic, G., Gernigon, L., Gaina, C., & Ball, P., 2012, Insights from the Jan Mayen system in the Norwegian–Greenland sea—I. Mapping of a microcontinent. Geophysical Journal International, 191, 385-412.
143. Peron-Pinvidic and Manatschal, 2010, From microcontinents to extensional allochthons: witnesses of how continents break apart?. Petroleum Geosciences, 16, 189–197, doi: 10.1144/1354-079309-903
144. Peyve, A. A., 2010, Tectonics and magmatism in eastern South America and the Brazil basin of the Atlantic in the Phanerozoic. Geotectonics, 44, 60-75.
145. Pichot, T., Delescluse, M., Chamot-Rooke, N., Pubellier, M., Qiu, Y., Meresse, F., Sun, G., Savva, D., Wong, K.P., Watremez, L., and Auxiètre, J. L., 2014, Deep crustal structure of the conjugate margins of the SW South China Sea from wide-angle refraction seismic data, Marine and Petroleum Geology, 58, 627-643.
146. Pindell, J. L., 1994, Evolution of the Gulf of Mexico and the Caribbean, in Donovan S.K. and Jackson, T. A. (eds.) Caribbean Geology: an introduction, University of the West Indies Publishers Association/University of the West Indies Press, Kingston, Jamaica, p. 13-39.
147. Pinheiro, L.M., Whitmarsh, R.B. and Miles, P.R., 1992. The ocean-continent boundary off the western margin of Iberia . Part II: crustal structure in the Tagus Abyssal Plain. Geophys. J. Int., 109, 106-124.
148. Planke, S., Symonds, P. A., Alvestad, E., & Skogseid, J., 2000, Seismic volcanostratigraphy of large-volume basaltic extrusive complexes on rifted margins. Journal of Geophysical Research, 105, 19335-19351.
149. Planke, S., & Eldholm, O., 1994, Seismic response and construction of seaward dipping wedges of flood basalts: Vøring volcanic margin. Journal of Geophysical Research, 99, 9263-9278.
150. Powell, C. M., Roots, S. R., & Veevers, J. J., 1988, Pre-breakup continental extension in East Gondwanaland and the early opening of the eastern Indian Ocean. Tectonophysics, 155, 261-283.
151. Rabinowitz, P. D., & LaBrecque, J. L., 1977, The isostatic gravity anomaly: key to the evolution of the ocean-continent boundary at passive continental margins. Earth and Planetary Science Letters, 35, 145-150.
152. Rabinowitz, P. D., & LaBrecque, J., 1979, The Mesozoic South Atlantic Ocean and evolution of its continental margins. Journal of Geophysical Research, 84, 5973-6002.
153. Raillard, S., 1990, Les marges de l'Afrique de l'Est et les zones de fracture associées: Chaine Davie et Ride du Mozambique, Campagne MD-60/MACAMO-II, Ph.D. thesis, 275 pp., Univ. Pierre et Marie Curie, Paris.
154. Ramana, M.V., Desa, M.A., and Ramprasad, T., 2015, Re-examination of geophysical data off Northwest India: Implications to the Late Cretaceous plate tectonics between India and Africa, Marine Geology, 365, 36—51, doi:10.1016/j.margeo.2015.04.002
155. Rao, D.G., Krishna, K.S, and Sar, D., 1997, Crustal evolution and sedimentation history of the Bay of Bengal since the Cretaceous, J. Geophys. Res., 102, 17747–17768, doi:10.1029/96JB01339.
156. Rao, G. S., & Radhakrishna, M., 2014, Crustal structure and nature of emplacement of the 85° E Ridge in the Mahanadi offshore based on constrained potential field modeling: Implications for intraplate plume emplaced volcanism. Journal of Asian Earth Sciences, 85, 80-96.
157. Reston, T. J., 1996, The S reflector west of Galicia: the seismic signature of a detachment fault. Geophysical Journal International, 127, 230-244.
158. Roest, W.R., and Srivastava, S.P., 1989, Sea-floor spreading in the Labrador Sea: A new reconstruction, Geology, 17, 1000—1003.

159. Roots, W. D., Veevers, J. J., & Clowes, D. F., 1979, Lithospheric model with thick oceanic crust at the continental boundary: a mechanism for shallow spreading ridges in young oceans, Earth and Planetary Science Letters, 43, 417-433.
160. Rosendahl, B. R., Meyers, J., Groschel, H., & Scott, D., 1992, Nature of the transition from continental to oceanic crust and the meaning of reflection Moho. Geology, 20, 721-724.
161. Ross, M. I., & Scotese, C. R., 1988, A hierarchical tectonic model of the Gulf of Mexico and Caribbean region. Tectonophysics, 155, 139-168.
162. Rowland, J. V., Baker, E., Ebinger, C. J., Keir, D., Kidane, T., Biggs, J., Hayward, N., and Wright, T. J., 2007, Fault growth at a nascent slow-spreading ridge: 2005 Dabbahu rifting episode, Afar. Geophysical Journal International, 171, 1226-1246.
163. Royer, J. Y., & Rollet, N., 1997, Plate-tectonic setting of the Tasmanian region. Australian Journal of Earth Sciences, 44, 543-560.
164. Royer, J.Y., and Sandwell, D.T., 1989, Evolution of the eastern Indian Ocean since the Late Cretaceous: Constraints from Geosat altimetry. Journal of Geophysical Research, 94, 13755-13782, doi: 10.1029/89JB01078
165. Sandwell, D. T., & Smith, W. H., 2009, Global marine gravity from retracked Geosat and ERS-1 altimetry: Ridge segmentation versus spreading rate. Journal of Geophysical Research, 114, B01411, doi:10.1029/2008JB006008.
166. Sandwell, D. T., Müller, R. D., Smith, W. H., Garcia, E., & Francis, R., 2014, New global marine gravity model from CryoSat-2 and Jason-1 reveals buried tectonic structure, Science, 346, 65-67.
167. Salvador, A., 1991, Origin and development of the Gulf of Mexico basin. The Gulf of Mexico Basin: Geological Society of America, Decade of North American Geology, v. J, 389-444.
168. Sawyer, D. S., Buffler, R. T., & Pilger Jr, R. H., 1991, The crust under the Gulf of Mexico Basin. In: *The Gulf of Mexico Basin: Geological Society of America, The Geology of North America, v. J*, 53-72.
169. Schouten, H., & Klitgord, K. D., 1994, Mechanistic solutions to the opening of the Gulf of Mexico. Geology, 22, 507-510.
170. Scott, R. A., 2000, Mesozoic-Cenozoic evolution of East Greenland: implications of a reinterpreted continent-ocean boundary location. Polarforschung, 68, 83-91.
171. Seifert, K.E., Chang, C.-W., and Brunotte, D.A., 1997, Evidence from Ocean Drilling Program Leg 149 mafic igneous rocks for oceanic crust in the Iberia Abyssal Plain ocean-continent transition zone, Journal of Geophysical Research, 102, 7915—7928.
172. Seton, M., Müller, R.D:, Zahirovic, S., Gaina, C., Torsvik, T., Shephard, G., Talsma, A., Gurnis, M., Turner, M., Maus, S., and Chandler, M., 2012, Global continental and ocean basin reconstructions since 200 Ma, Earth Science Reviews, 113, 212-270, doi:10.1016/j.earscirev.2012.03.002
173. Singh, S.C., Crawford, W.C., Carton, H., Seher, T., Combier, V., Cannat, M., Canales, J.P., Düsünür, D., Escartin, J., and Miranda, J.M., 2006, Discovery of a magma chamber and faults beneath a Mid-Atlantic Ridge hydrothermal field. Nature, 442, 1029-1032.
174. Singh, S.C., Harding, A.J., Kent, G.M., Sinha, M.C., Combier, V., Bazin, S., Tong, C.H., Pye, J.W., Barton, P.J., Hobbs, R.W., White, R.S., & Orcutt, J. A., 2006, Seismic reflection images of the Moho underlying melt sills at the East Pacific Rise. Nature, 442, 287-290.
175. Sinha, S. T., Nemcok, M., Choudhuri, M., Misra, A.A., Sharma, S.P., Sinha, N., & Venkatraman, S., 2010, The crustal architecture and continental break up of East India Passive margin: an integrated study of deep reflection seismic interpretation and gravity modeling. In AAPG Annual Convention & Exhibition, New Orleans, USA, CD-ROM.
176. Skaarup, N., Jackson, H. R., and Oakey, G., 2006, Margin segmentation of Baffin Bay/Davis Strait, eastern Canada based on seismic reflection and potential field data. Marine and Petroleum Geology, 23, 127-144.
177. Skogseid, J., Pedersen, T., Eldholm, O., & Larsen, B.T., 1992, Tectonism and magmatism during NE Atlantic continental break-up: the Vøring Margin. Geological Society, London, Special Publications, 68, 305-320. doi: 10.1144/GSL.SP.1992.068.01.19
178. Small, C., 1998. Global systematics of mid-ocean ridge morphology, in Faulting and Magmatism at Mid-Ocean Ridges, Vol. 106, pp. 1–25, eds Buck, W.R., Delaney, P.T., Karson, J.A. & Lababrielle, Y., American Geophysical Union Monograph.
179. Sreejith, K. M., Krishna, K. S., and Bansal, A. R., 2008, Structure and isostatic compensation of the Comorin Ridge, north central Indian Ocean. Geophysical Journal International, 175, 729-741.
180. Srivastava, S.P., Sibuet, J.C., Cande, S., Roest, W.R., and Reid, I.D., 2000. Magnetic evidence for slow seafloor spreading during the formation of the Newfoundland and Iberian margins. Earth and Planetary Science Letters 182, 61–76.

181. Stagg, H. M. J., and Willcox, J. B., 1992, A case for Australia-Antarctica separation in the Neocomian (ca. 125 Ma), Tectonophysics, 210, 21-32.
182. Stagg, H. M. J., Colwel, J. B., Direen, N. G., O'Brien, P. E., Bernardel, G., Borissova, I., Brown, B., and Ishirara, T., 2004, Geology of the continental margin of Enderby and Mac. Robertson Lands, East Antarctica: insights from a regional data set. Marine Geophysical Researches, 25, 183-219.
183. Subrahmanyam, V., Subrahmanyam, A. S., Murty, G. P. S., & Murthy, K. S. R., 2008, Morphology and tectonics of Mahanadi Basin, northeastern continental margin of India from geophysical studies. Marine Geology, 253, 63-72.
184. Suckro, S. K., Gohl, K., Funck, T., Heyde, I., Ehrhardt, A., Schreckenberger, B., Gerlings, J., Damm, V., and Jokat, W., 2012, The crustal structure of southern Baffin Bay: implications from a seismic refraction experiment. *Geophysical Journal International*, *190*, 37-58.
185. Sutra, E., Manatschal, G., Mohn, G., and Unternehr, P., 2013, Quantification and restoration of extensional deformation along the Western Iberia and Newfoundland rifted margins, Geochem. Geophys. Geosyst., 14, 2575–2597, doi:10.1002/ggge.20135.
186. Tasrianto, R., and Escalona, A., 2015, Rift architecture of the Lofoten-Vesterålen margin, offshore Norway, Marine and Petroleum Geology, 64, 1-16. http://dx.doi.org/10.1016/j.marpetgeo.2015.02.036
187. Thinon, I., Matias, L., Réhault, J. P., Hirn, A., Fidalgo-González, L., & Avedik, F. (2003). Deep structure of the Armorican Basin (Bay of Biscay): a review of Norgasis seismic reflection and refraction data. Journal of the Geological Society, 160, 99-116.
188. Tiberi, C., Ebinger, C., Ballu, V., Stuart, G., & Oluma, B., 2005, Inverse models of gravity data from the Red Sea-Aden-East African rifts triple junction zone, Geophysical Journal International, 163, 775-787.
189. Todal, A., & Eldholm, O., 1998, Continental margin of western India and Deccan large igneous province: Marine Geophysical Research, 20, 273-291.
190. Todd, B., Reid, I., Keen, C., 1988. Crustal structure across the southwest Newfoundland transform margin. Canadian Journal of Earth Sciences 25, 744–759.
191. Torsvik, T. H., Rousse, S., Labails, C., & Smethurst, M. A., 2009, A new scheme for the opening of the South Atlantic Ocean and the dissection of an Aptian salt basin. Geophysical Journal International, 177, 1315-1333.
192. Tsikalas, F., Eldholm, O., & Faleide, J. I., 2002, Early Eocene sea floor spreading and continent-ocean boundary between Jan Mayen and Senja fracture zones in the Norwegian-Greenland Sea. Marine Geophysical Researches, 23, 247-270.
193. Tucholke, B.E., Sibuet, J.-C., Klaus, A., et al., 2004, Proc. ODP, Init. Repts., 210: College Station, TX (Ocean Drilling Program). doi:10.2973/odp.proc.ir.210.2004
194. Tucholke, B. E., Sawyer, D. S., & Sibuet, J. C., 2007, Breakup of the Newfoundland–Iberia rift. Geological Society, London, Special Publications, 282, 9-46.
195. Veevers, J. J., 2009, Palinspastic (pre-rift and-drift) fit of India and conjugate Antarctica and geological connections across the suture. Gondwana Research, 16, 90-108.
196. Veevers, J. J., Tayton, J. W., & Johnson, B. D., 1985, Prominent magnetic anomaly along the continent-ocean boundary between the northwestern margin of Australia (Exmouth and Scott plateaus) and the Argo abyssal plain. Earth and planetary science letters, 72, 415-426.
197. Veevers, J.J., 1987, The conjugate continental margins of Antarctica and Australia, in The Antarctic Continental Margin: Geology and Geophysics of Offshore Wilkes Land, Earth Sci. Ser., vol. 5A, Eittreim, S.L., and Hampton, M.A. (eds), pp 45-73, Circum Pacific Conference for Energy and Mineral Resources, Houston, Texas.
198. Vorren, T. O., Richardsen, G., Knutsen, S. M., & Henriksen, E., 1991, Cenozoic erosion and sedimentation in the western Barents Sea. Marine and Petroleum Geology, 8, 317-340.
199. Voss, M., & Jokat, W., 2007, Continent-ocean transition and voluminous magmatic underplating derived from P-wave velocity modelling of the East Greenland continental margin. Geophysical Journal International, 170, 580-604.
200. Voss, M., Schmidt-Aursch, M. C., & Jokat, W., 2009, Variations in magmatic processes along the East Greenland volcanic margin. Geophysical Journal International, 177, 755-782.
201. Wang, T., Chen, M., Lee, C., and Xia, K., 2006, Seismic imaging of the transitional crust across the northeastern margin of the South China Sea, *Tectonophysics*, 412, 237–254, doi:10.1016/j.tecto.2005.10.039
202. Watts, A. B., & Fairhead, J. D., 1999, A process-oriented approach to modeling the gravity signature of continental margins. The Leading Edge, 18, 258-263.
203. Wegener, A., 1915, Die Entstehung der Kontinente und Ozeane, Vieweg und Sohn, Braunschweig, Germany.

204. White, R. S., Detrick, R. S., Mutter, J. C., Buhl, P., Minshull, T.A., and Morris, E., 1990, New seismic images of oceanic crustal structure: Geology, 18, 462–465.
205. White, R. S., Minshull, T. A., Bickle, M. J., & Robinson, C. J., 2001, Melt generation at very slow-spreading oceanic ridges: Constraints from geochemical and geophysical data. Journal of Petrology, 42, 1171-1196.
206. Whitmarsh, R. B., and P. R. Miles, 1995, Models of the development of the West Iberia rifted continental margin at 40°30′N deduced from surface and deep-tow magnetic anomalies, J. Geophys. Res., 100, 3789–3806, doi:10.1029/94JB02877.
207. Whitmarsh, R.B., Sawyer, D.S., Klaus, A., and Masson, D.G. (Eds.), 1996. Proc. ODP, Sci. Results, 149: College Station, TX (Ocean Drilling Program). doi:10.2973/odp.proc.sr.149.1996
208. Whitmarsh, R.B., Manatschal, G., and Minshull, T.A., 2001, Evolution of magma-poor continental margins from rifting to seafloor spreading, Nature, 413, 150—154.
209. Whittaker, R.C., Hamann, N.E., and Pulvertaft, T.C.R., 1997, A new frontier province offshore northwest Greenland: Structure, basin development, and petroleum potential of the Melville Bay area, AAPG Bulletin, 81, 978-998.
210. Wildman, M., Brown, R., Watkins, R., Carter, A., Gleadow, A., and Summerfield, M., 2015, Post break-up tectonic inversion across the southwestern cape of South Africa: New insights from apatite and zircon fission track thermochronometry, Tectonophysics, 654, 30—55 http://dx.doi.org/10.1016/j.tecto.2015.04.012.
211. Williams, S. E., Whittaker, J. M., & Müller, R. D., 2011, Full-fit, palinspastic reconstruction of the conjugate Australian-Antarctic margins. Tectonics, 30, TC6012, doi:10.1029/2011TC002912.
212. Winker, C. D., & Buffler, R. T., 1988, Paleogeographic evolution of early deep-water Gulf of Mexico and margins, Jurassic to Middle Cretaceous (Comanchean). AAPG Bulletin, 72, 318-346.
213. Wolfenden, E., Ebinger, C., Yirgu, G., Renne, P. R., & Kelley, S. P., 2005, Evolution of a volcanic rifted margin: Southern Red Sea, Ethiopia. Geological Society of America Bulletin, 117, 846-864.
214. Zhu, J., Qiu, X., Xu, H., Zhan, W., Zhao, M., Wei, X., Sun, J., Yang, R., Xia, S., and Huang, H., 2012, Seismic reflection characteristic and structure unit division of an ocean-continent transition zone in the northern South China Sea. Journal of Tropical Oceanography, 31, 28-34

Figures

Figure 1. Interpretation, after Stagg et al. (2004), of a COB from seismic reflection data at the Antarctic margin of the Indian Ocean. Seismic data from the SCAR seismic data library system (http://www.scar-sdls.org).

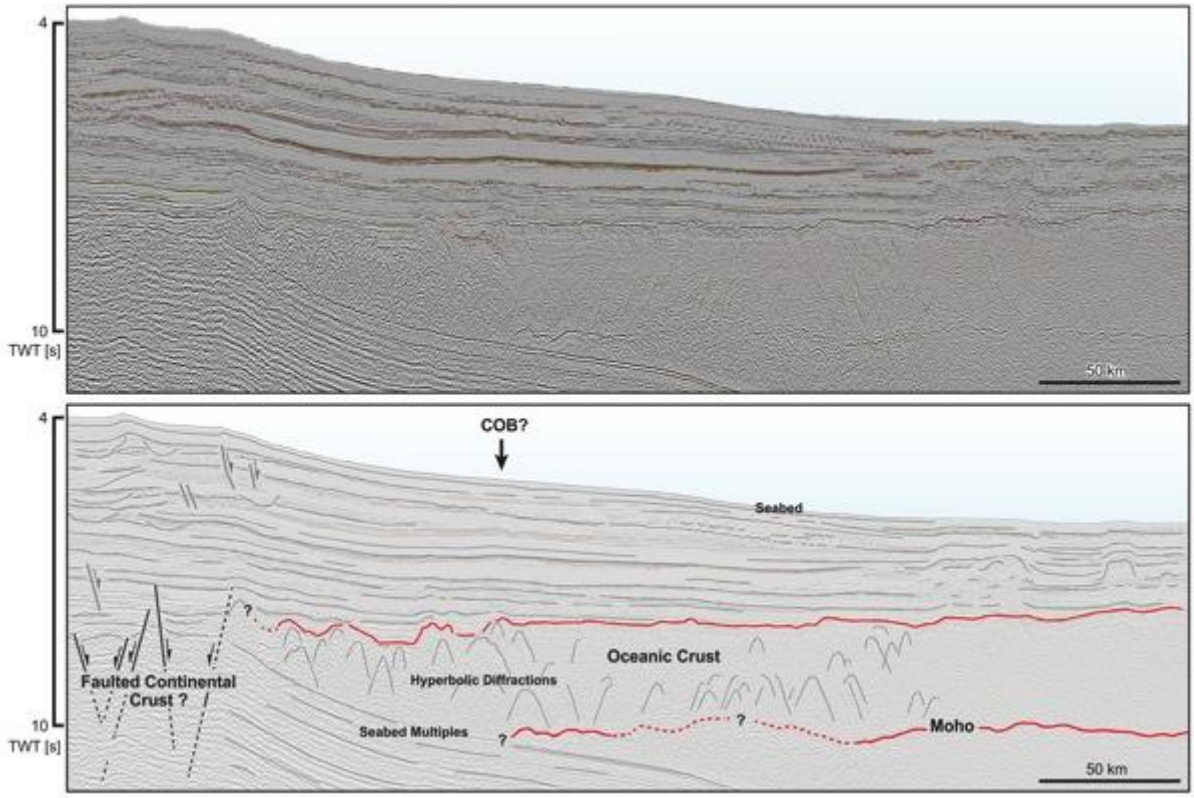

Figure 2. Interpretation of seaward dipping reflectors in seismic reflection data from the Namibian continental margin. Seismic data courtesy of CGG (formerly CGGVeritas) and the Virtual Seismic Atlas (http://www.seismicatlas.org).

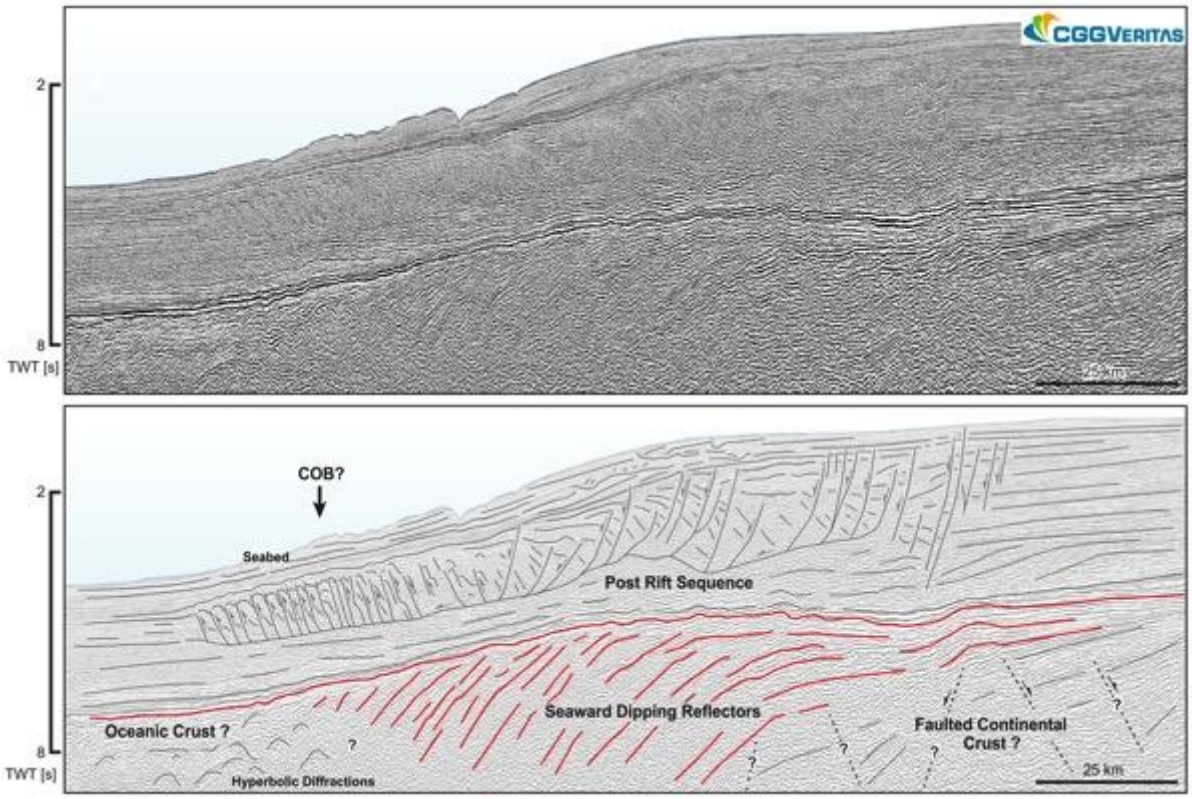

Figure 3. Top: a refraction profile based on OBS data from the extended margin east of Greenland, redrawn and simplified from Voss et al. (2007). In profiles like this, definitive oceanic crust may be taken to be represented by a layer with consistent properties of thickness around 7 km and velocities 6.6—6.8 kms^{-1}, overlying either a base-of-crust reflection (e.g. as at 300-400 km) or a faster layer interpreted as mantle material (e.g. as at 100-200 km). Bottom: Refraction data used in a network of sonobuoy velocity profiles for Leitchenkov et al's (2014) COB interpretation in the Indian Ocean sector of Antarctica. The velocities shown are for the first sub-basement layer, in which velocities of 5.8—6.2 kms^{-1} were taken as diagnostic of oceanic crust (purple disks) and velocities of 4.4—5.6 kms-1 were taken to diagnose continental crust (orange disks). The green envelope suggests the kind of uncertainty in COB location that might be expected from interpolating a COB within such a data set (n.b. Leitchenkov et al. (2014) also used seismic reflection and potential field data to locate their COB (green line)).

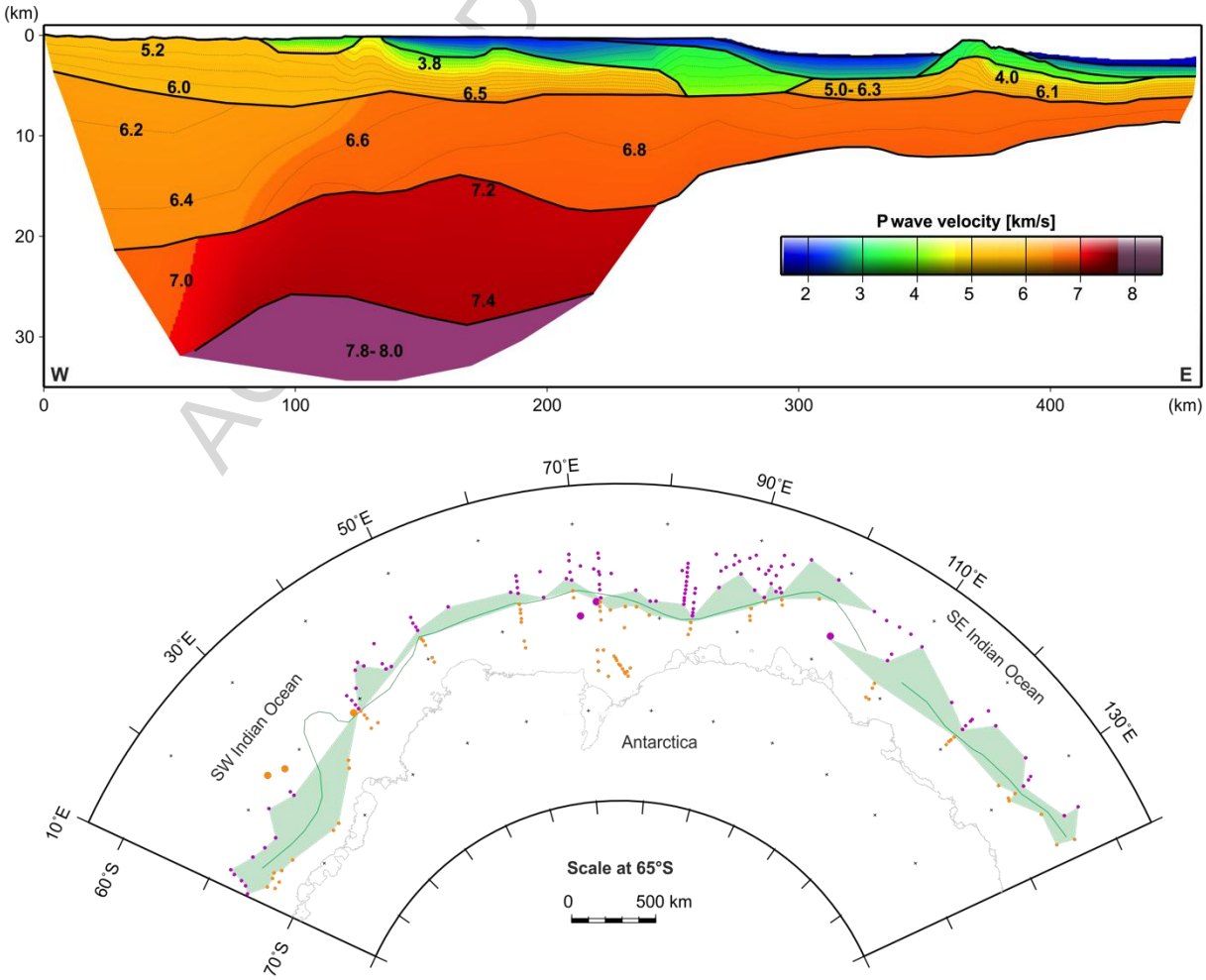

Figure 4. Picking uncertainty (pink) in magnetic anomaly profiles (all from the NGDC's online archive: https://www.ngdc.noaa.gov/mgg/geodas/trackline.html). Left: In N-S oriented profiles over normal oceanic crust formed at slow spreading rates in profiles south of Australia at ~30°S, the steep limb of a magnetic reversal anomaly might be picked with an uncertainty of 5-10 km. Right: in spite of the E-W orientation of profiles at a similar latitude off the Namibian continental margin, which for identical sources would produce simpler anomaly waveforms than at the Australian margin, a COB that might be interpreted at the feather edge of basalts in the margin's SDR sequence is consistently more difficult to pinpoint from the magnetic anomaly, with uncertainty in the region of 20-50 km.

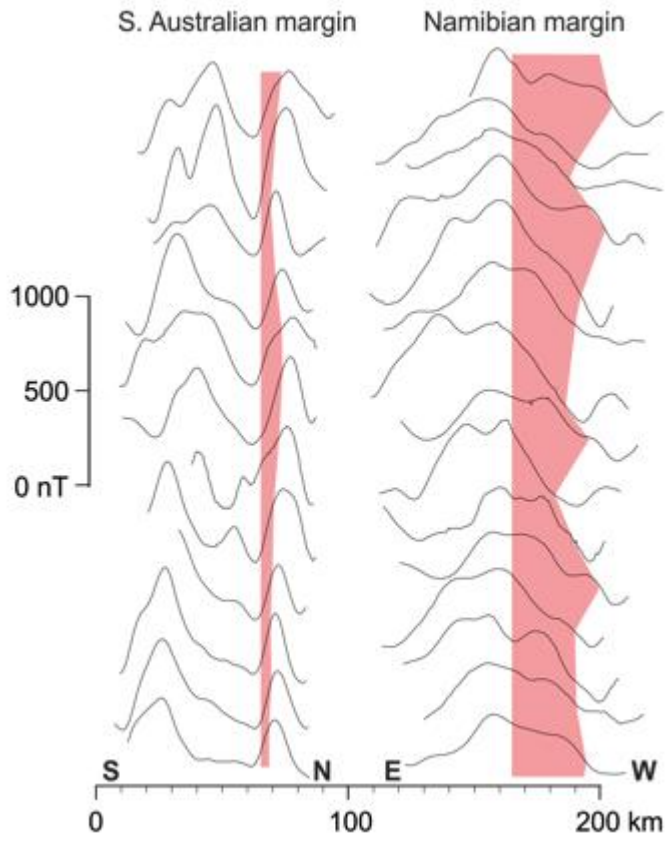

Figure 5. Top: Modification of an extended continental margin and neighbouring oceanic crust (green) by sedimentation (yellow) or magmatic underplating (violet) and accompanying flexure for an elastic thickness of 20 km. Depending on these few processes, the COB (dashed line) might be interpreted from a seaward free-air gravity low, the landward gradient behind it, or the landward gradient behind the gravity high associated with the shelf break. Adapted from figures in Watts and Fairhead (1999). Bottom: Comparison of picking uncertainties (pink) for a COB in gravity anomalies from an extended continental margin (A-A′; ~150 km) and of a fracture zone trough in gravity anomalies (B-B′; ~5-10 km). Gravity grid data from Sandwell et al. (2014).

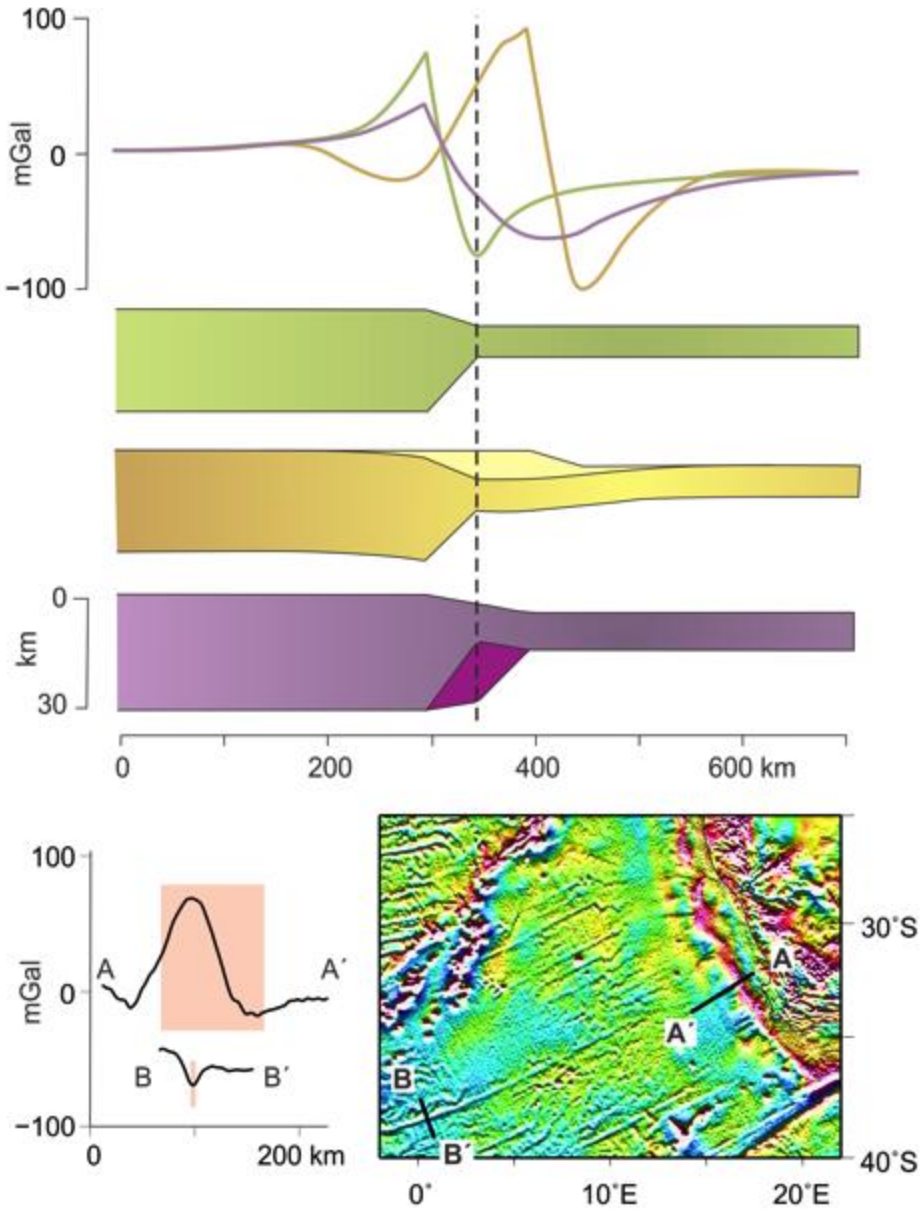

Figure 6. Ensemble of COB estimates at the extended margins of the Gulf of Mexico. Background images in this figure and Figures 7—12 show gridded free-air gravity anomalies of Sandwell et al. (2014). COB estimate sources are 1: Sawyer et al. (1991); 2: Marton and Buffler (1994); 3: Pindell (1994); 4: Schouten and Klitgord (1994); 5: Bird et al. (2005); 5b: envelope of previous estimates from Bird et al. (2005); 6: Bouysse et al. (2009); 7: Seton et al. (2012); 8: Hudec et al. (2013); 9: Christeson et al. (2014); 10: Sandwell et al. (2014).

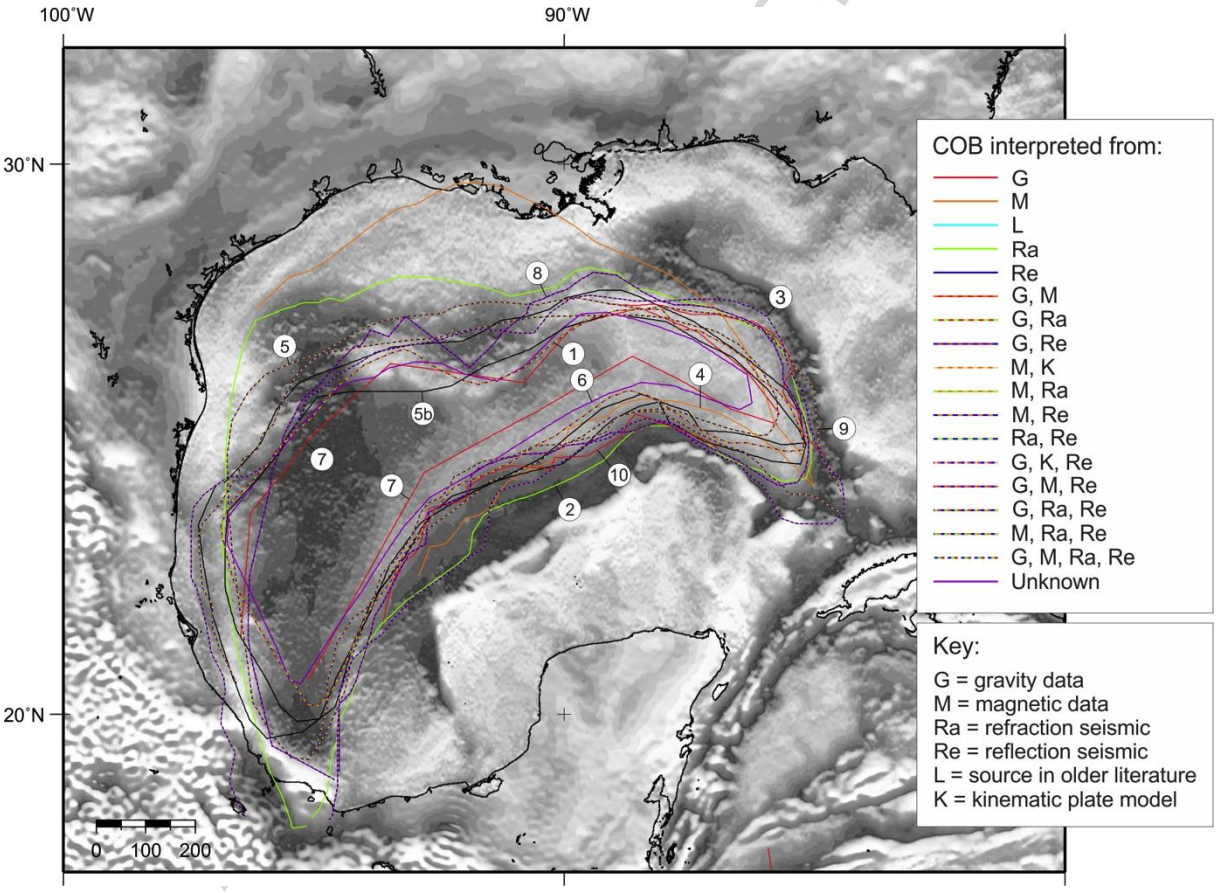

Figure 7. Ensemble of COB estimates at the extended margins of Antarctica bordering the Indian Ocean. Key to colours as for Figure 5. COB estimate sources are 1: Powell et al. (1988); 2: Royer and Sandwell (1989); 3: Eittreim (1994); 4: Ishihara et al. (1999); 5: Gaina et al. (2003); 6: Stagg et al. (2004); 7: Gaina et al. (2007); 8: Gohl et al. (2008); 9: Bouysse et al. (2009); 10: Close et al. (2009); 11: Leitchenkov et al. (2009); 12: Direen et al. (2011); 13: Seton et al. (2012); 14: Ball et al. (2013); 15: Nogi et al. (2013); 16: Leitchenkov et al. (2014); 17: Gillard et al. (2015).

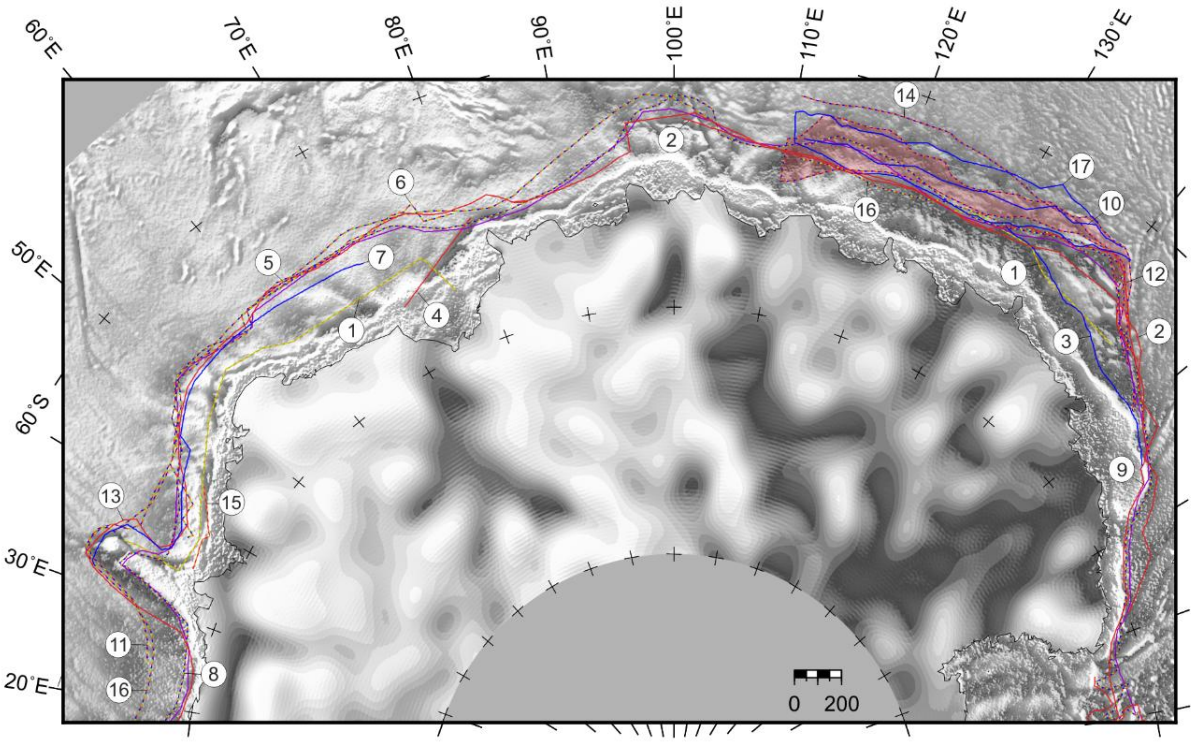

Figure 8. Ensemble of COB estimates at the extended margins of Australia. Key to colours as for Figure 5. COB estimate sources are 1: Veevers et al. (1985); 2: Veevers et al. (1987); 3: Powell et al. (1988); 4: Fullerton et al. (1989); 5: Royer and Sandwell (1989); Stagg and Wilcox (1992); 7: Exon et al. (1996); 8: Royer and Rollet (1997); 9: Gaina et al. (1998); 10: Brown et al. (2003); 11: Norvick (2004); 12: Heine and Müller (2005); 13: Müller et al. (2005); 14: Norvick et al. (2008); 15: Bouysse et al. (2009); 16: Direen et al. (2011); 17: Williams et al. (2011); 18: Seton et al. (2012); 19: Ball et al. (2013); 20: Hall et al. (2013); 21: Gillard et al. (2015).

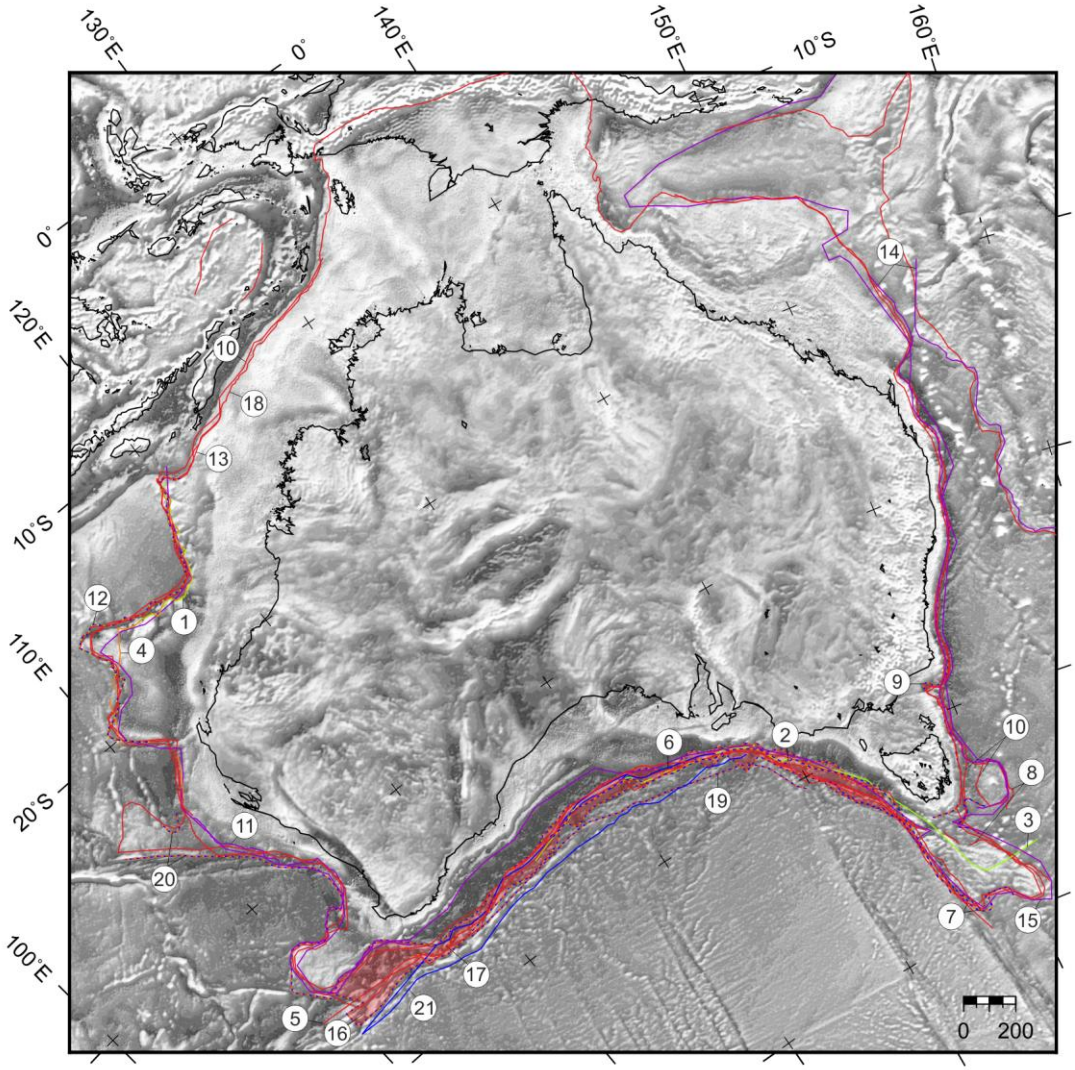

Figure 9. Ensemble of COB estimates at the extended margins bordering the South China Sea. Key to colours as for Figure 5. COB estimate sources are 1:Briais et al. (1993); 2: Nissen et al. (1995); 3: Hsu et al. (2004); 4: Wang et al. (2006); 5: Bouysse et al. (2009); 6: Hu et al. (2009); 7: Deng et al. (2012); 8: Li et al. (2012); 9: Seton et al. (2012); 10: Zhu et al. (2012); 11. Barckhausen et al. (2014); 12: Chen et al. (2014); 13: Hwang and Chang (2014); 14: Pichot et al. (2014); 15: Bai et al., 2015; 16: Cameselle et al. (2015); 17: Li et al. (2015).

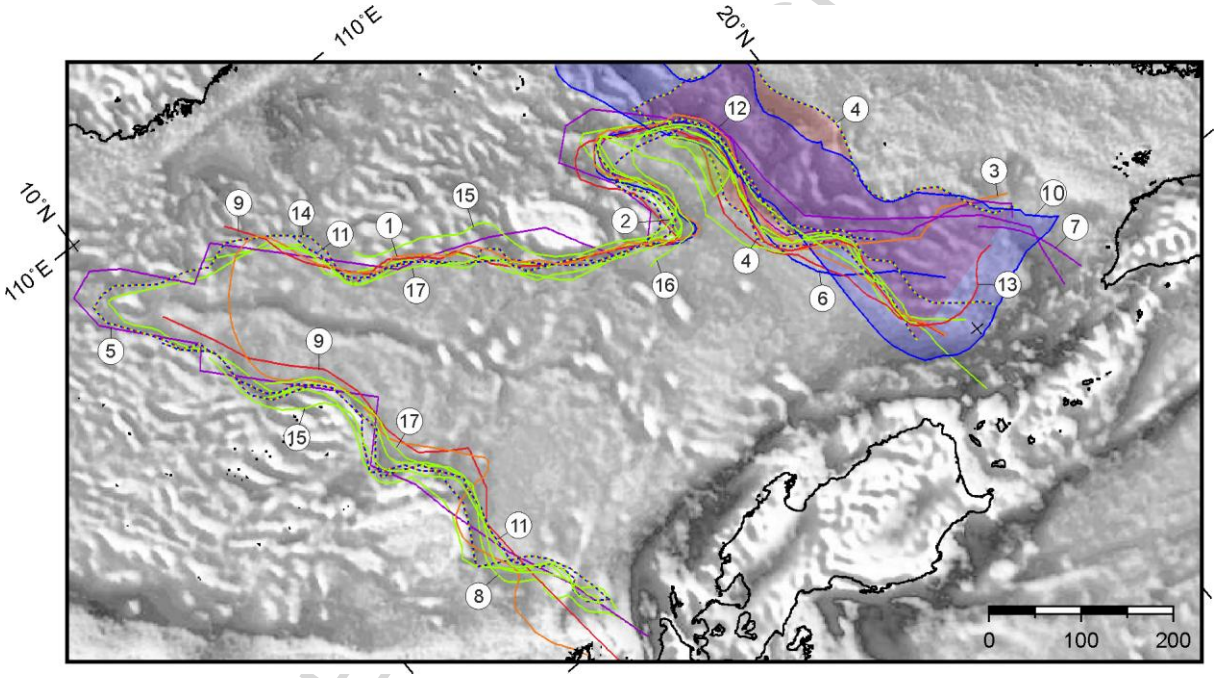

Figure 10. Ensemble of COB estimates at the extended continental margins bordering the Northern Indian Ocean. Key to colours as for Figure 5. COB estimate sources are 1: Naini and Talwani (1982); 2: Powell et al. (1988); 3: Rao et al. (1997); 4: Malod et al. (1997); 5: Todal and Eldholm (1998); 6: Calvès et al. (2008); 7: Sreejith et al. (2008); 8: Subrahmanyam et al. (2008); 9: Bouysse et al. (2009); 10: Krishna et al. (2009); 11: Veevers (2009); 12: Bastia et al. (2010); 13: Corfield et al. (2010); 14: Sinha et al. (2010); 15: Calvès et al. (2011); 16: Arora et al. (2012); 17: Seton et al. (2012); 18: Gibbons et al. (2013); 19: Nemčok et al. (2013); 20: Rao and Radhakrishna (2014); 21: Minshull et al. (2015); 22: Ramana et al. (2015).

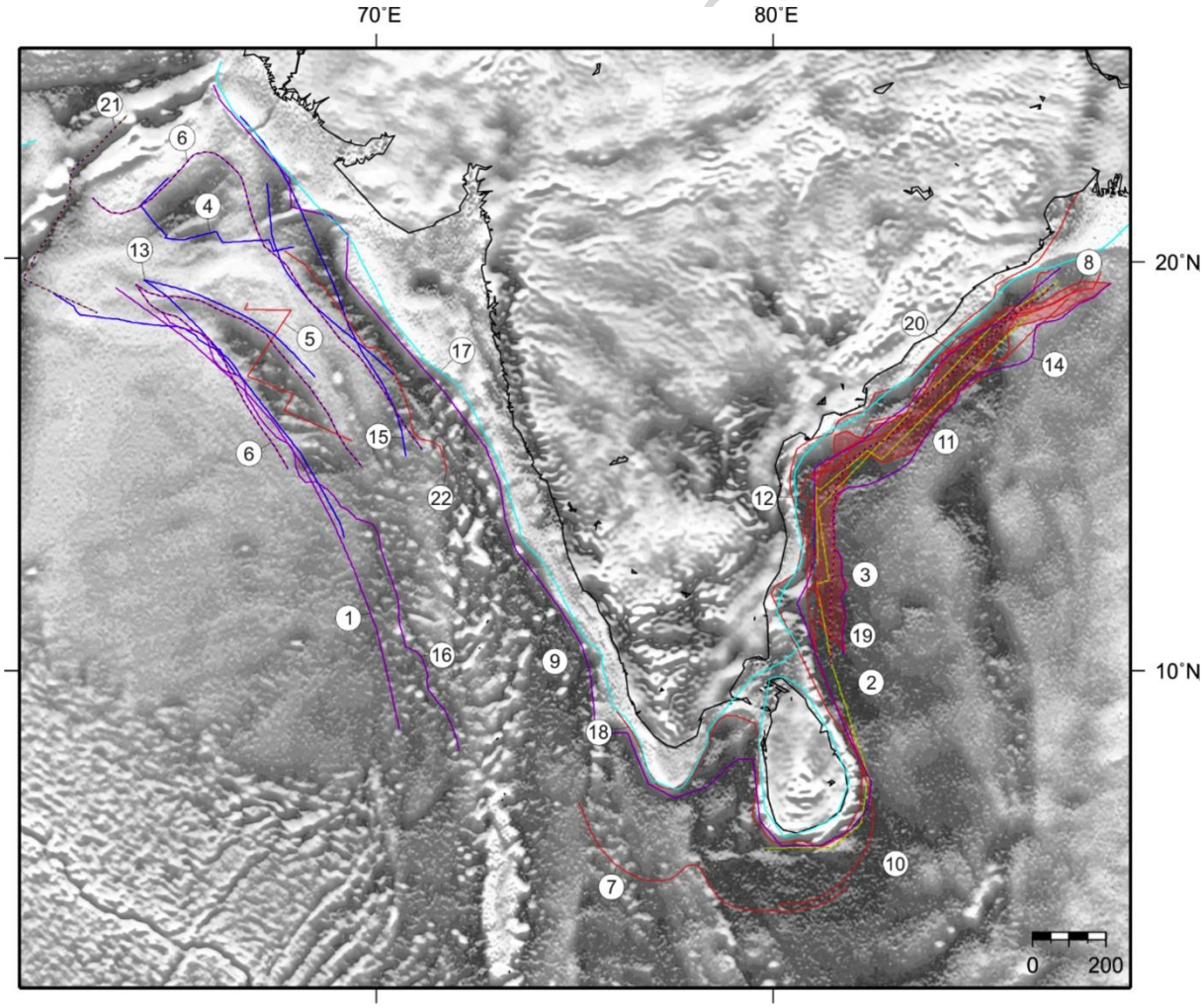

Figure 11. Ensemble of COB estimates at the extended margins bordering the North Atlantic. Key to colours as for Figure 5. COB estimate sources are 1: Dunbar and Sawyer (1985); 2: Boillot and Winterer (1988); 3: Roest and Srivastava (1989); 4: Todd et al. (1988); 5: Faleide et al. (1991); 6: Vorren et al. (1991); 7: Skogseid et al. (1992); 8: Keen and Dehler (1993); 9: Escher and Pulvertaft (1995); 10: Whittaker et al. (1997); 11: Eldholm (1998); 12: Breivik et al. (1999); 13: Scott (2000); 14: Srivastava et al. (2000); 15: Holbrook (2001); 16: Mosar et al. (2002); 17: Tsikalis et al. (2002); 18: Thinon et al. (2003); 19: Kimbell et al. (2005); 20: Lundin and Doré (2005); 21: Naylor and Shannon (2005); 22: Engen et al. (2006); 23: Skaarup et al. (2006); 24: Olesen et al. (2007); 25: Tucholke et al. (2007); 26: Voss and Jokat (2007); 27: Engen (2008); 28: Mjelde et al. (2008); 29: Bouysse et al. (2009); 30: Gaina et al. (2009); 31: Voss et al. (2009); 32: Peron-Pinvidic and Manatschal (2010); 33: Libak et al. (2012); 34: Peron-Pinvidic (2012); 35: Seton et al. (2012); 36: Suckro et al. (2012); 37: Oakey et al., (2013); 38: Hosseinpour et al. (2013); 39: Gernigon et al. (2015); 40: Tasrianto and Escalona (2015).

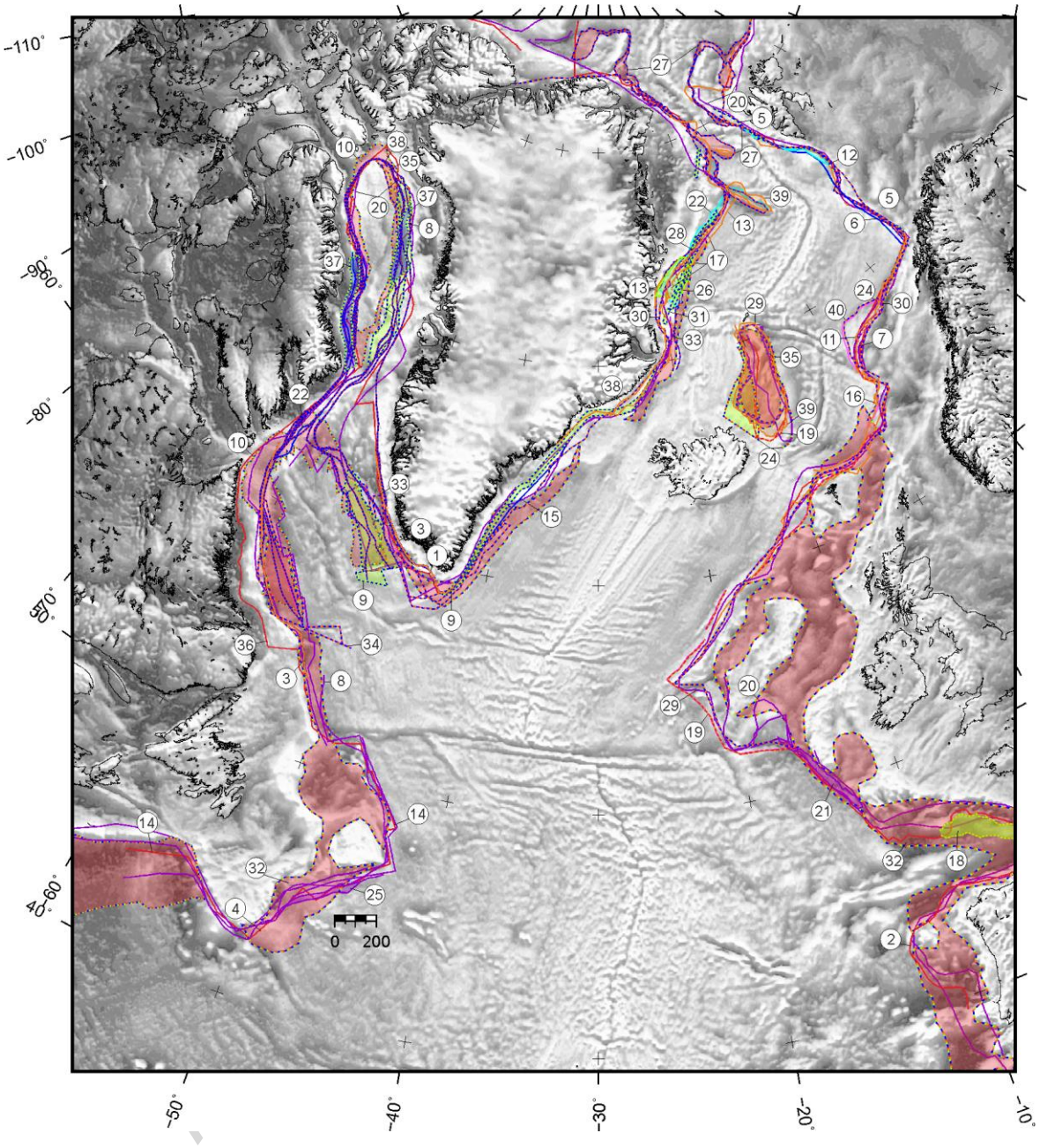

Figure 12. Ensemble of COB estimates at the extended margins bordering the South Atlantic. Key to colours as for Figure 5. COB estimate sources are 1: Rabinowitz and LaBrecque (1979); 2: Austin and Uchupi (1982); 3: Raillard (1990); 4: Nürnberg and Müller (1991); 5: Chang (1992); 6: Light et al. (1993); 7: Gladczenko et al. (1997); 8: Lawver et al. (1998); 9: Cainelli and Mohriak (1999); 10: Karner and Driscoll (1999); 11: Bauer et al. (2000); 12: Macdonald et al. (2003); 13: König and Jokat (2006); 14: Blaich et al. (2008); 15: Pawlowski (2008); 16: Bouysse et al. (2009); 17: Torsvik et al. (2009); 18: Anka (2010); 19: Labails et al. (2010); 20: Peyve (2010); 21: Seton et al. (2012); 22: Gaina et al. (2013); 23: Heine et al. (2013); 24: Wildman et al., 2015.

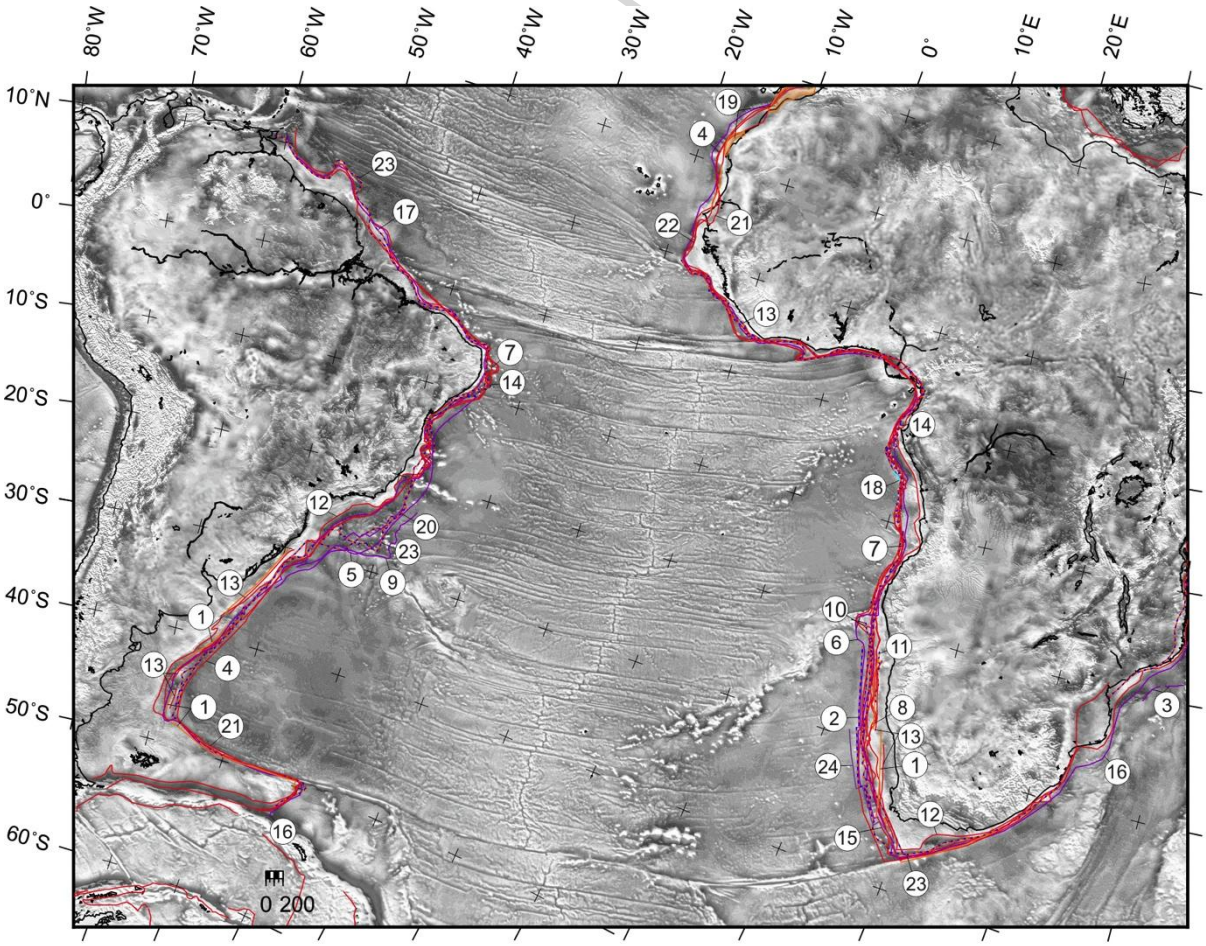

Figure 13. Publication chronology for COB estimates in our ensembles. COB estimates are classified by location and year of publication. Coloured bars at the bottom of the plot indicate the publication period over which the maximum width of the ensemble at each margin (Table 1) was achieved.

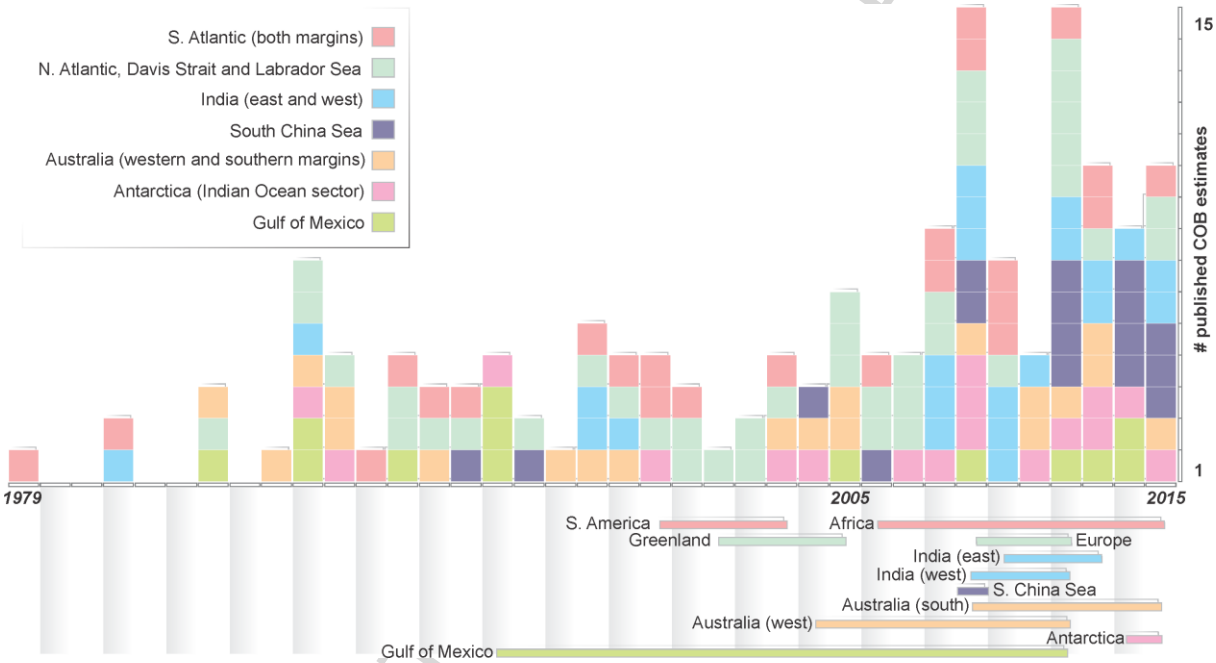

Figure 14. Implausible precision in the results of palinspastic modelling. Palinspastic restorations of extreme estimates of the COB location from the ensemble in the Cape Basin, off South Africa (black dashed lines) give an estimate of the region in which the 'pre-stretching COB' may have lain (blue envelope). Modelling uses crustal stretching factors determined using a pre-stretching crustal thickness of 35 km and the CRUST1.0 data set (http://igppweb.ucsd.edu/~gabi/rem.html), with no allowance for igneous addition to the COTZ. The zone of extended continental crust is assumed to lie between the COB and an inland limit at the red dashed line. Plate divergence is assumed to have occurred by partial rotation about the FIT-M5no stage pole of Pérez-Díaz and Eagles (2014). Pink ellipses show that 95% uncertainty regions for the location of three points rotated into the restored region by a full rotation about that pole exceed the range of restored COB locations. Uncertainties of partial rotations about this pole, if they could be calculated, would be larger still, and thus larger than the width of the restored ensemble. Background shows the shelf-related free-air gravity anomaly (Sandwell et al., 2014), to which the restored COB ensemble is a close match.

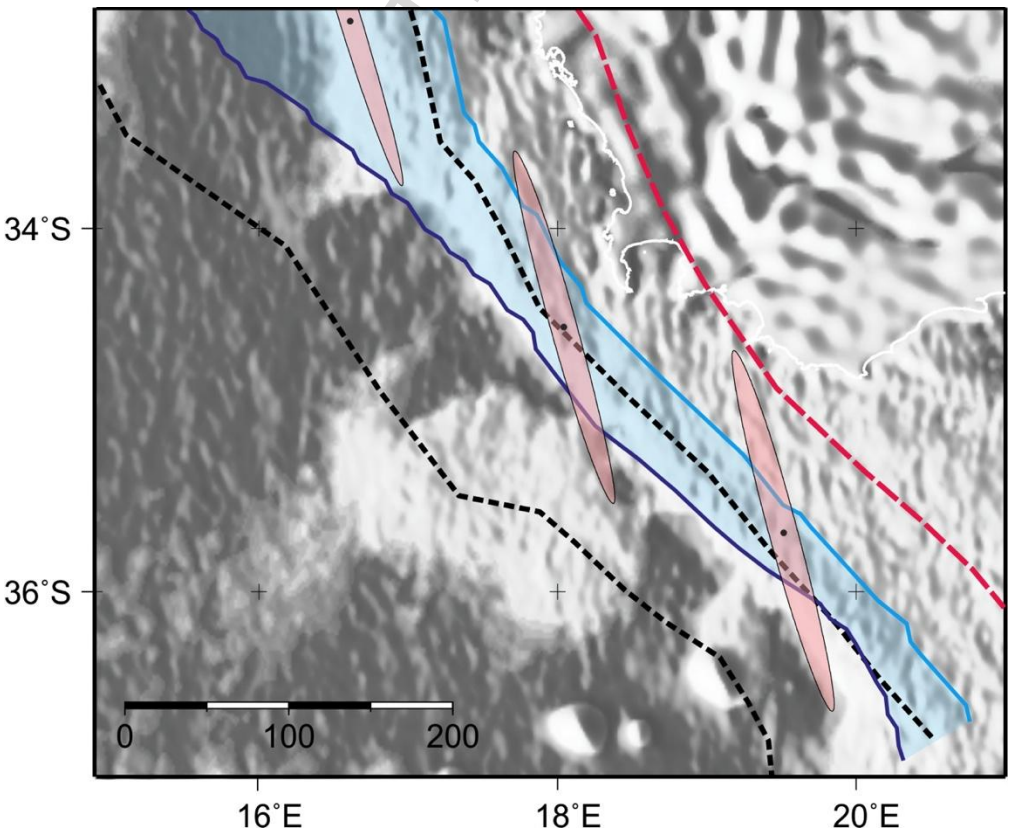

Figure 15. Use of COB ensembles (dark blue on African plate, pale blue on South American plate after rotation to Africa) in plate kinematic modelling. Heavy dashed lines indicate breaks in the South American ensemble used to fit the COBs interpreted as multiple isochronous segments. Misfit refers to the total area enclosed by COBs in the reconstructions. Assuming equal likelihood of any of the COB estimates being correct within the uncertainties discussed in the text, the kinematic scenarios shown must be regarded as three equally plausible bases for making end-rift stage reconstructions of the South Atlantic.

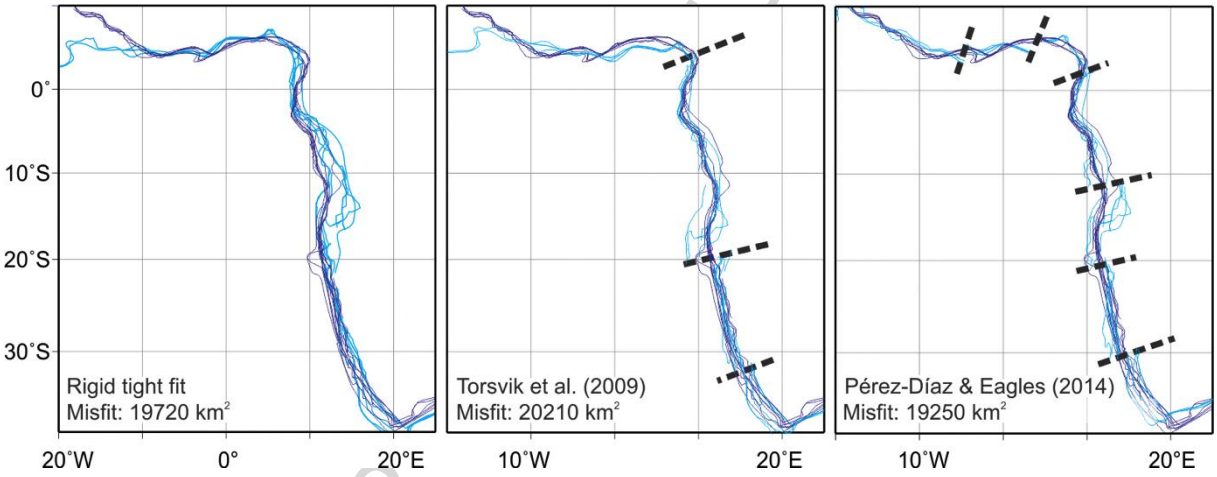

Table 1. Summary of COB estimate ensemble statistics

Margin/Ensemble	*# COB or COTZ estimates*	*# ensemble width measurements*	*Mean width (km)*	*Standard deviation of widths (km)*	*Maximum width (km)*
India (west)	14	7	475	90	668
South Atlantic (west)	11	23	217	194	816
Antarctica (Indian ocean sector)	17	19	206	93	366
Australia (south)	11	18	187	80	265
India (east)	8	16	184	79	429
Magma rich[1,2]	76	50	182	153	668
Magma poor[1,3]	80	81	175	87	386
South Atlantic (east)	13	21	179	68	293
Gulf of Mexico	16	33	153	86	382
Labrador Sea & Davis Strait	14	30	149	84	386
North Atlantic (east)	14	30	148	125	398
North Atlantic (west)	15	25	136	94	356
S. China Sea	17	29	118	92	317
Australia (west)	9	15	86	110	476
Global	**159**	**266**	**167**	**120**	**816**

[1]measurements only on those margin segments classified by Boillot and Coulon (1998) that are also characterized by ensembles in this study.
[2]Labrador Sea & Davis Strait, Newfoundland, Iberia, Bay of Biscay, southern Ireland and southwestern UK, Pelotas, Congo, southern Australia and Wilkes Land, Antarctica.
[3]Greenland, north Ireland to Norway, Argentine and Cape basins, west of India, NW Australia.